VI-2186

PL-TR-93-2232

REVIEW OF THE CLDSIM CLOUD RADIANCE SIMULATOR

Ross J. Thornburg
John G. DeVore
James Thompson

Visidyne, Inc.
10 Corporate Place
So. Bedford Street
Burlington, MA 01803

15 December 1993

Final Report
26 September 1990-31 October 1994

PHILLIPS LABORATORY
Directorate of Geophysics
AIR FORCE MATERIEL COMMAND
HANSCOM AIR FORCE BASE, MA 01731-3010

DISCLAIMER NOTICE

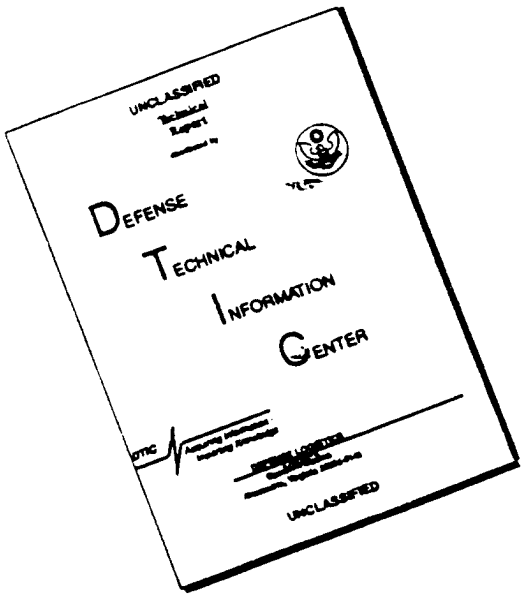

THIS DOCUMENT IS BEST QUALITY AVAILABLE. THE COPY FURNISHED TO DTIC CONTAINED A SIGNIFICANT NUMBER OF PAGES WHICH DO NOT REPRODUCE LEGIBLY.

This technical report has been reviewed and is approved for publication

FRANCIS X. ROBERT
Contract Manager

STEPHAN D. PRICE
Branch Chief

ROGER VAN TASSEL
Division Director

This report has been reviewed by the ESC Public Affairs Office (PA) and is releasable to the National Technical Information Service (NTIS).

Qualified requestors may obtain additional copies from the Defense Technical Information Center. All others should apply to the National Technical Information Service.

If your address has changed, or if you wish to be removed from the mailing list, or if the addressee is no longer employed by your organization, please notify PL/TSI, Hanscom AFB, MA 01731-3010. This will assist us in maintaining a current mailing list.

Do not return copies of this report unless contractual obligations or notices on a specific document requires that it be returned.

REPORT DOCUMENTATION PAGE

Form Approved
OMB No. 0704-0188

1. AGENCY USE ONLY (Leave blank)	2. REPORT DATE	3. REPORT TYPE AND DATES COVERED
	15 December 1993	Final (26 September 1990–31 October 1994)

4. TITLE AND SUBTITLE

Review of the CLDSIM Cloud Radiance Simulator

5. FUNDING NUMBERS

C-F19628-90-C-0187
PE 63220C
PR 5321
TA 06 WUAB

6. AUTHOR(S)

Ross J. Thornburg, John G. DeVore, James H. Thompson

7. PERFORMING ORGANIZATION NAME(S) AND ADDRESS(ES)

Visidyne, Inc.
10 Corporate Place
So. Bedford Street
Burlington, MA 01803

8. PERFORMING ORGANIZATION REPORT NUMBER

VI-2186

9. SPONSORING / MONITORING AGENCY NAME(S) AND ADDRESS(ES)

Phillips Laboratory
29 Randolph Road
Hanscom AFB, MA 01731-3010
Contract Manager: Frank Robert/GPOB

10. SPONSORING / MONITORING AGENCY REPORT NUMBER

PL-TR-93-2232

11. SUPPLEMENTARY NOTES

12a. DISTRIBUTION / AVAILABILITY STATEMENT

Approved for public release, distribution unlimited.

12b. DISTRIBUTION CODE

13. ABSTRACT *(Maximum 200 words)*

Visidyne has conducted an independent review of CLDSIM, a cloud model resident in the SSGM code. CLDSIM simulates cloud background, a major source of clutter for IR sensors viewing from space. An evaluation of CLDSIM, along with recommendations for possible improvement are presented. (The version of CLDSIM reviewed corresponds to that in the SSGM Release 5.1).

14. SUBJECT TERMS

BRDF NORSE CLDSIM Cloud Radiance Modeling
MSLAB SSGM Optical Sensor

15. NUMBER OF PAGES

68

16. PRICE CODE

17. SECURITY CLASSIFICATION OF REPORT	18. SECURITY CLASSIFICATION OF THIS PAGE	19. SECURITY CLASSIFICATION OF ABSTRACT	20. LIMITATION OF ABSTRACT
UNCLASSIFIED	UNCLASSIFIED	UNCLASSIFIED	UL

Table of Contents

List of Tables

List of Figures

Executive Summary

Through thermal emission and scattered solar radiation, clouds present a significant clutter source to infrared surveillance sensors viewing from space. To simulate these effects for the defense community, Photon Research Associates (PRA) has developed CLDSIM. This program has been used to generate cloud background scenes both as a stand-alone code and as a part of the Strategic Scene Generation Model (SSGM). Since the SSGM is gaining acceptance as a standard source of background radiance scenes for defense simulations, it is important to review CLDSIM to understand what it does and how it can be improved.

This report presents an independent review of CLDSIM undertaken by Visidyne, Inc. To accomplish its task, Visidyne has generated cloud images with CLDSIM; inspected available documentation, briefings and validation reports; read through the code; and had several discussions with PRA. The discussions focused on the current operation of CLDSIM and future development plans.

Chapter 1 of the report gives a brief overview of CLDSIM code and of the databases that it requires to operate. Chapter 2 reviews each of CLDSIM's components in turn. A description of each component is followed by a critique with recommended changes. A list of PRA's planned changes is also given. Chapter 3 describes the MSLAB code that Visidyne developed to calculate scattering off of clouds. This code is used to investigate the limits of CLDSIM's treatment of this process. Chapter 4 presents a calculation of the effects of line correlations between gaseous absorbers in the cloud and in the surrounding atmosphere. This calculation provides an explanation of a factor of three difference between CLDSIM's calculations and data in an absorbing region. Chapter 5 provides a table listing recommended improvements to CLDSIM. Chapter 6 concludes with a list of references.

CLDSIM Version

The term CLDSIM properly refers to a specific PRA proprietary code that calculates cloud radiances that are displayed as a scene viewed from a sensor's perspective. Over time, the term has come to represent, first, a collection of PRA stand-alone codes that perform a range of auxilliary functions necessary to prepare inputs for CLDSIM proper, and second, the SSGM implementation of these codes. The stand-alone codes and the SSGM implementation differ enough that PRA calls the latter SSGM CLOUD / HORIZON. The SSGM implementation differs from the stand-alone version by being about one release

behind the stand-alone code, by having a few parameters hardwired, and by having fewer databases to access. Visidyne reviewed SSGM CLOUD / HORIZON Release 5.1. Throughout most of this report, it is simply called CLDSIM, because that is the more general name used in the defense community, and because many of the comments made about the SSGM implementation pertain as well to the stand-alone version of the code corresponding to Release 5.1. Lists of databases and BRDFs given below should not be taken as limitations on the number available. New capabilities of the stand-alone code can be inferred from the descriptions of PRA's plans for Release 6.0 and beyond.

CLDSIM Operation

CLDSIM models infrared cloud radiances by combining blackbody thermal emissions at cloud altitude with solar radiation scattered from the cloud's top surface. To perform its calculations, CLDSIM requires

(1) Databases of cloud top altitudes to determine the temperature at which the cloud top radiates, as well as descriptions of the scattering properties of the cloud droplets.

(2) Databases of Bidirectional Reflectance Distribution Functions (BRDFs) which determine the magnitude and direction of light scattered off of the cloud surface.

(3) APART radiation transport code calculations of the spectral solar irradiance, path radiance, and skyshine observed by a sensor.

CLDSIM operates by looping over the pixels of a cloud database, determining altitudes and calculating scattering geometries. The APART radiances are interpolated over altitude, and over bounding solar and observer positions. The interpolated temperature of the cloud top as well as the interpolated cloud emissivity are used to calculate the cloud's thermal emission, while the BRDF and solar irradiance determine the solar scattered radiance. Path radiance, skyshine, and transmitted radiance from the underlying terrain are also include.

Databases

In SSGM Release 5.1, CLDSIM is supplied with a set of seventeen cloud top altitude databases to use in simulations. These are generated from such sources as NOAA satellite multispectral infrared data. Cloud altitudes are computed by assuming that the cloud surface radiates as a blackbody at the local atmospheric temperature. The apparent brightness

values from cloud images are thus converted into local temperatures, while atmospheric profiles obtained from coincident sounding measurements provide a means to convert from temperature to altitude. Altitude thresholds and visual inspection of the data are used to type the observed clouds as being either altostratus with 4 km base, altostratus with 6km base, cumulonimbus, or cirrus.

Only clouds represented in one of CLDSIM's cloud altitude databases can be included in a CLDSIM simulation. Therefore, it is important to know how representative these databases are, both in terms of the types of clouds represented, and in the range of radiances that CLDSIM predicts from them. The databases generally have been created at the request of one of several project offices that has chosen a particular scenario to run over a particular location. PRA has then been tasked to inspect the available data and to create cloud altitude databases that are representative of stressing cloud conditions for the scenario. One can thus say that CLDSIM covers the range of clouds for the particular locations of these scenarios. To broaden the range of clouds available to the general user, PRA has added several new databases over the past few years. There is presently no metric to confirm that a spanning set of cloud types has been obtained, or that the CLDSIM cloud returns span the range of returns observed by sensors. Extensive data from a platform such as DSP would be needed to generate such a metric.

Users desire CLDSIM databases that have both high spatial resolution and wide coverage. These two requirements are often in conflict. Many of CLDSIM's databases have been created using the wide coverage of NOAA satellites. These databases come from data with the moderate resolution of 1.1 km. To obtain higher resolution data, PRA interpolates this data down to a resolution of 200 - 400m using a complicated process of elliptical fits and PSD filtering. The assumption behind the PSD filtering, namely that the cloud spatial structure is scale invariant over the range 10 km to 200m, has been criticized as not validated. PRA has also been seeking higher resolution satellite and aircraft data that do not require interpolation. Sources of high resolution, low coverage data should be used where applicable. However, there is still a need to provide high resolution databases with wide extent. Thus, the current method of interpolation should be validated, or new methods developed. Fractal or wavelet methods might be useful here. In addition, cloud interpolation techniques might lead to statistical descriptions of cloud tops that would allow synthetic generation of cloud databases to supplement those derived from measurements.

Several assumptions are involved in transforming apparent brightness maps into cloud altitudes. The accuracy of these assumptions should be tested against stereoscopic

measurements of cloud tops, if such data exists.

BRDFs

CLDSIM is supplied with four BRDFs which represent scattering off of spherical scatterers in two altostratus water clouds, a cumulonimbus water/ice cloud, and a cirrus ice cloud. A separate model exists for specular scattering off of aligned platelets in a cirrus cloud. The precomputed BRDFs are generated using a Mie scattering code and an adding and doubling method treatment to determine the angular distribution of radiation scattered off of a horizontally homogeneous slab with a given distribution of scatterer sizes and a given thickness. The BRDFs represent optically thick clouds, which tend to have rather smooth angular distributions of scattered radiation. Although CLDSIM models optically thin clouds by apply a correction that reduces the overall magnitude of the scattered radiance, it does not adjust the angular distribution of scattering. It thus does not model such effects as rainbows. CLDSIM's treatment of scattering should be improved to produce such effects, either by interpolating on optical depth between the single scattering BRDF and the optically thick BRDF, or by adopting methods developed in Chapter 3. In that chapter a method is developed to approximate BRDFs for many particle distributions very quickly. If this method were employed, it would increase the diversity of cloud scattering in CLDSIM.

Calculational Steps

CLDSIM does a good job calculating radiances from clouds, especially for nadir viewing geometries. As the viewer goes to lower elevation angles, the treatment becomes poorer, largely due to deficiencies in cloud-on-cloud interactions. CLDSIM handles shadowing on the cloud surface locally. A pixel is in shadow or not depending on its orientation to the sun and the viewer. The shadowing of one part of the cloud by another is not treated. The illumination of part of the cloud by radiation scattered off of another part is handled only diffusely, as an multiplicative correction to the surface's own radiance. The shadowing treatment in CLDSIM should be upgraded, perhaps by using low resolution renderings of the cloud to provide shadows and illumination for the higher resolution pixels of the final image. A current revision of the code will improve CLDSIM's shadowing techniques, but it must be finished before it can be evaluated.

CLDSIM assumes that scattering is a surface effect, rather than a volume effect. This is true if the mean free path for scattering is small compared to the radius of curvature of the cloud. Because they are calculated for thick slab geometries, CLDSIM's BRDFs may not do

as well calculating radiances from "puffs" in a cumulus cloud as they do predicting radiances from a stratus deck. Other geometries should be considered in calculating BRDFs.

Two other areas need improvement. Currently, CLDSIM footprints cloud pixels onto a cylinder that curves away from the sensor, rather than onto a portion of a sphere. There are plans to upgrade this in the coming years. In addition, CLDSIM uses beam transmission equations that may underestimate the amount of ground clutter that passes through clouds.

CLDSIM in the SSGM

CLDSIM is increasingly being used as an element of the SSGM rather than as a stand-alone code. The SSGM environment poses new difficulties that do not exist when CLDSIM is run by an experienced user as a stand-alone code. A complex mixture of geometries, cloud databases, BRDFs and atmospheric profiles must be assembled to produce any CLDSIM run. This mixture needs to be assembled in a physically self-consistent manner. The implementation of CLDSIM in the SSGM tries to aid the user by making certain choices automatically. For instance, the correct BRDFs are determined in the SSGM when the cloud databases are chosen. While this is a good start, it does not go far enough it keeping the inexperienced user from creating an unphysical cloud image inadvertently. Nor is there sufficient information supplied with a cloud image to inform a general user when non-standard cloud parameters are used by an experienced user. For instance, during the recent BASS review, CLDSIM images were created using an arctic atmosphere with equatorial clouds to increase contrast. This fact became less well known as the images were transmitted from person to person. More information should be provided to the user to aid in constructing consistent cloud images and more error checking should be added to the code. A way to keep warnings about non-standard cloud scenes with the images should be developed.

CLDSIM has an architecture that sequentially processes whole databases, one step at a time. For instance, CLDSIM calculates pixel scattering geometries for millions of pixels in a databases, even if only a few of them are in the FOV. To reduce the large run times this produces, a "cookie cutter" utility is being developed for the SSGM to allow the user to create a small cloud database from a section of a large cloud database. This is part of a revision of CLDSIM to meet faster processing goals in the SSGM. Adopting a pixel-oriented architecture for the revision, rather than a database-oriented one, may improve CLDSIM's performance even more.

Visidyne's MSLAB Routine

To check the BRDF treatment in CLDSIM, Visidyne adapted Mie and slab scattering routines used in the NORSE nuclear weapons effect code to produce MSLAB. The technical details of this code are given in Chapter 3. MSLAB's Mie code is able to calculate accurate scattering patterns for both small and large scatterers. The slab scattering treatment in MSLAB calculates the single scattering BRDF for a slab of arbitrary thickness, and adds to it an estimate of the multiple scattering contribution. Validation runs show that MSLAB does a good job calculating scattering patterns, and that it reproduces the variation of BRDFs with optical depth and particle size. MSLAB includes a simple model of gaseous absorption inside the cloud that could be easily upgraded to provide better results.

MSLAB is a fast running code. It could be used in a general cloud modeling code to provide BRDFs for a wide range of cloud droplet distributions and optical thicknesses. A slight modification of the code would allow it to predict scattering off of surfaces with small radii of curvature.

Line Correlation Transmission Effects

CLDSIM calculates transmissions by multiplying the transmission through a cloud with the transmission of the surrounding atmosphere. Line correlations between gaseous absorbers in the cloud and in the atmosphere make this a poor approximation in important absorbing regions. A calculation is presented in Chapter 4 showing that treating transmissions as uncorrelated can produce an underprediction of the transmission by a factor of 30 at around 2.7 μm for a 5 km altitude cloud and by a factor of 3 for an 11 km cloud. These calculations provide an explanation for a difference between CLDSIM predictions and data.

Conclusions

A table of conclusions and recommendations is provided in Chapter 5.

1. INTRODUCTION

Through thermal emission and scattered solar radiation, clouds present a significant clutter source to infrared surveillance sensors viewing from space. To simulate these effects for the defense community, Photon Research Associates (PRA) has developed over a series of years a powerful cloud radiance simulation program called CLDSIM. This program has been used to generate cloud background scenes for contractors developing new sensors. It is also a major component of the Strategic Scene Generation Model (SSGM). The SSGM is gaining acceptance as a standard source of background radiance scenes for defense simulations. CLDSIM is becoming a standard source of cloud backgrounds along with it.

Because of the central role CLDSIM is assuming in providing backgrounds to the defense community, it has been the subject of several reviews recently, both internally at PRA and externally. This paper reports on a comprehensive review of CLDSIM that Visidyne was tasked to undertake. This review has benefited from the cooperation of PRA, but it has been independent of that company. It differs from previous external reviews of CLDSIM by examining not only CLDSIM's results, but the code itself, along with much of the available documentation on CLDSIM.

As a way of introduction, Section 1.1 briefly describes the major components of CLDSIM. Section 1.2 describes the methodology Visidyne employed to review CLDSIM.

1.1 Overview of CLDSIM

Narrowly defined, CLDSIM refers to a PRA developed routine that models infrared cloud radiances. It does so by combining the blackbody thermal emissions at cloud altitudes with solar radiation scattered from the cloud's top surface. CLDSIM requires many sources of data to perform its calculations. It uses databases of cloud altitudes to determine the temperature at which the cloud top radiates, as well as descriptions of the scattering properties of the cloud droplets. It also takes as inputs descriptions of the incident solar radiance, along with skyshine and path radiance. Broadly defined, CLDSIM refers to a set of codes that are used together to provide the information required to produce cloud radiance scenes. The major components are

(1) Several proprietary PRA routines that transform measured cloud images into databases of cloud top altitudes;

(2) PRA's proprietary Multiple Scattering and Radiation Transport (MSRAT) code that

computes the scattering characteristics of clouds as expressed through Bidirectional Reflectance Distribution Functions (BRDFs);

(3) The APART code that supplies solar irradiance, thermal and solar skyshine, and thermal and solar path radiance to CLDSIM for specified geometries and at a high spectral resolution;

(4) The CLDSIM code that takes inputs from these other codes and produces cloud radiance scenes.

Although CLDSIM exists as a stand-alone code at PRA and a few other locations, most users encounter CLDSIM as part of the SSGM. Running CLDSIM in the SSGM is similar to running CLDSIM alone, except that (1) the SSGM version of CLDSIM generally lags the PRA version of the code by about one release, and (2) some of CLDSIM's options have been hardwired to predetermined values in the SSGM implementation. For instance, CLDSIM has the capability to add an offset to the cloud altitude databases, which can alter the predicted cloud radiances by moving the clouds to a different temperature level and by changing the amount of absorbing atmosphere above the cloud. In addition, PRA has routinely generated cloud images for customers with stand-alone CLDSIM that differ from those produced through the SSGM by coming from a cloud altitude database not distributed with the SSGM, by having more or different cloud types represented, or by having BRDFs representative of different scattering conditions. Many of the limitations found in the SSGM version of CLDSIM are actually implemented through simple entries into SSGM text files. Thus, a determined user could reclaim much of the extra functionality of the corresponding stand alone version of CLDSIM by editing a few files (to move the cloud altitude offset for instance), or by acquiring the extra databases and BRDFs. Since the general user will encounter CLDSIM through the SSGM and will not alter its implementation there, this review will only deal with the capabilities found in the standard SSGM version of CLDSIM. While the formal name for this version is CLOUD / HORIZON in SSGM Release 5.1, it will be referred to as CLDSIM in this review.

Before CLDSIM is delivered to the SSGM, cloud top altitude databases are generated from such sources as NOAA satellite data. This is done assuming that the measured apparent brightnesses can be converted into the temperature of a blackbody radiator, and that an atmospheric profile giving temperature as a function of altitude can be constructed from other data. Currently seventeen such cloud altitude databases are available in the SSGM to simulate clouds. In addition, MSRAT is run to generate BRDF databases which

give the reflected radiance resulting from a unit incident irradiance as a function of angle and wavelength. Since scattering patterns depend on the size of the scatterer, these databases depend on the distribution of cloud droplet radii. In the SSGM, four BRDFs are available to simulate altostratus clouds at 4 km cloud base, altostratus clouds at 6 km cloud base, as well as cumulonimbus and cirrus clouds.

To run CLDSIM in the SSGM, the user specifies which cloud altitude database to use and its position on the earth. The solar position is computed from the time input, and the user specifies the observer location. Given these inputs, APART is run to provide radiance levels at eleven altitudes. CLDSIM then loops over each of the pixels in the cloud altitude database to determine the local cloud altitude and orientation. The altitude and cloud emissivity are used to determine the blackbody radiance from the pixel, as well as to interpolate the APART outputs. Scattering angles are computed with respect to the pixel's surface normal, and the BRDF is combined with the interpolated solar irradiance to give the scattered radiance. To complete the calculation, radiances are combined to form the total radiance, and then footprinted into the viewer's perspective.

It should be noted that in the SSGM the user does not run CLDSIM directly, but creates an SSGM input file outlining the scenario of interest, and starts the SSGM's execution. The SSGM creates the correct input files for CLDSIM and APART, obtains the radiance output, and combines it with other scenario elements to produce a final scene. The cloud altitude databases and the BRDFs are supplied with the SSGM.

1.2 Visidyne Methodology

Because Visidyne is a developer of one of the components of the SSGM, Visidyne personnel had general familiarity with CLDSIM and its operation before this review began. To complete this study Visidyne took the following steps:

(1) Read through the computer code for CLDSIM and several of its auxiliary routines;
(2) Examined available manuals, briefings and validation reports;
(3) Interviewed PRA about specific features of CLDSIM; and
(4) Performed independent cloud radiance calculations as a check on CLDSIM.

The outline of this report is as follows. In Section 2, a description of each of the major CLDSIM components is presented, followed by a brief critique. Previous validations of CLDSIM by PRA and others are mentioned. This study has focused on the version of CLDSIM that was available in the last release of the SSGM, Release 5.1. Since that release,

the SSGM has undergone extensive revision as it changes from its Baseline Phase to its Operational Phase. Several corresponding changes to CLDSIM have been made or are being planned. To show how CLDSIM is developing, planned PRA changes to CLDSIM are listed for each component.

Two sets of independent calculations are presented in this report. Because solar scattering is a significant contributor to cloud clutter, an evaluation of the BRDFs used in CLDSIM has been a major activity of this review. A model for solar scattering was adapted from Visidyne's NORSE code, and BRDFs were calculated for comparison to CLDSIM's. A full description of the model and the results is provided in Section 3. In Section 4, different methods are presented for handling line correlations between transmission in a cloud and in the surrounding atmosphere. These calculations give an explanation for a discrepancy between CLDSIM predictions and data. Recommendations and conclusions make up Section 5.

2. DESCRIPTION OF CLDSIM

CLDSIM models the thermal emission and solar-scattered radiance of clouds as observed by satellite-borne sensors. CLDSIM works by combining the databases of cloud altitudes with surface reflection data and radiation transport equations to produce the cloud radiance scene. Each of these components will be described below. Each description is followed by a critique of the methods used in CLDSIM. Improvements that PRA plans to make to the code are also listed. These plans come from (Mertz, 1993) and (Shanks and Mertz, 1993), as well as from discussions with PRA personnel.

2.1 Cloud Altitude Databases

The overall features that one sees in a CLDSIM image come from the information that is contained in one of CLDSIM's cloud altitude databases. (See Table 1 for a list of the seventeen databases supplied with the SSGM.) The process of creating these databases from satellite data is well described by Mertz (Mertz, 1991a), who delineates the steps taken to create CLDSIM databases for use in BSTS studies. The steps are

(1) Acquire radiometric images of clouds and atmospheric temperature profiles;
(2) Convert cloud brightnesses to altitudes assuming blackbody radiation;
(3) Determine cloud types; and
(4) Resize the database to the desired resolution.

Three databases were constructed for the BSTS study using archived data from the Advanced Very High Resolution Radiometer (AVHRR) aboard NOAA-9. This instrument images in five bands with an average resolution of 1.1 km. Coincident temperature measurements were obtained by the TOVS sounding product, which has a footprint of around 17 km. The TOVS data gives layer-mean temperatures at a given location as a function of pressure in 15 layers. This data is used to form a piece-wise continuous temperature profile as a function of altitude, using hydrostatic equilibrium and the ideal gas equation. The AVHRR radiometric data is then converted to altitude measurements assuming that the cloud top is a blackbody radiating at a temperature corresponding to the measured apparent brightness. The atmospheric temperature profile is applied to each pixel's blackbody temperature to produce a final cloud top altitude. Different temperature profiles are used for different pixel groups to account for changes in temperature due to weather fronts or geographic boundaries.

The AVHRR databases contain non-cloud features that must be removed. Visual inspection of the multispectral data is done to identify underlying land, ice and water. A mask is then created to remove them from further consideration. The remaining pixels in the images are classified by cloud type. In the SSGM, the types are altostratus with 4 km altitude base, altostratus with 6 km base, cumulonimbus and cirrus. This is based on brightness thresholds, which translate into altitude differences. This manual typing is checked using statistical measures of the altitudes for each cloud. Corrections to cloud altitudes are made to account for dimmer apparent brightnesses at thin cloud edges. Also, when one cloud covers another, the boundaries between the clouds are altered to make the correct join. Two databases representing the cloud result from this work. One gives cloud top altitude as a function of position, and the other contains a code identifying the cloud type of each pixel.

Quite often users want cloud databases finer than the 1.1 km resolution of the AVHRR. In the past, PRA has employed a cloud interpolation scheme to produce resolutions of 200 or 400 meters. This technique involves taking each row of the altitude database and finding all minima and maxima. Ellipses are fit between extrema in such a way that maxima have zero slope while minima are cusps. These ellipses are then evaluated at the desired resolution. The columns of the altitude database are similarly fit and interpolated, and the two sets of altitudes are averaged. Because this process creates artifacts in the database, the PSD of the database is formed and filtered to removed spikes. The filtering is designed to produce a PSD with the same $k^{-\alpha}$ roll-off behavior for the high frequencies corresponding to the new interpolated values as was observed in the highest frequencies of the original

data. This implements PRA's assumption that cloud spatial structure is scale invariant from 10 km to 200m. The inverse transform of the PSD produces the final altitude database. The resolution of the cloud type database is increased to match that of the altitude database.

TABLE 1. Cloud databases available in the SSGM

Database	Cloud Types (from Assigned BRDFs)	Number of Pixels (Millons)	Pixel Size (m)	EW x NS Extent (km)
alto/test	cumulo	0.016	400	51 x 51
CIRRUS/EQUATORIAL	cirrus	2.2	120	180 x 177
CUMNIMB/TROP	cumulo	1.05	400	410 x 410
BAJA	alto6, cumulo, cirrus	1.05	120	123 x 123
CIRRUS/MONSOON	cirrus	2.2	120	180 x 177
ALTOSTRAT/MIDLAT	alto6	1.05	400	410 x 410
CIRROSTRAT/MIDLAT	cirrus	1.05	400	410 x 410
OCEAN/MIDLAT	alto6, cumulo, cirrus	31.90	200	573 x 2228
STRATOCUM/MIDLAT	alto6	2.3	120	188 x 176
STRATUS_STREETS	alto6	1.05	120	123 x 123
SILOFIELDS	alto6, cumulo, cirrus	3.42	200	205 x 668
VASSA	alto6, cumulo, cirrus	50	200	800 x 2500
KIJEV	alto6, cumulo, cirrus	46.8	200	800 x 2340
KIJEV_NORTH	alto6, cumulo, cirrus	24	200	800 x 1200
BALTIC	alto4, cumulo	0.0655	1000	256 x 256
ALTOCUM/POLAR	alto6	5.12	30	31 x 150
CUMNIMB/POLAR	cumulo	5.12	30	31 x 150

Critique of the Databases

CLDSIM's databases can be evaluated in terms of their spatial coverage and resolution, and in terms of how well they span the collection of clouds that one might encounter. Users generally request databases with fine spatial resolution and wide area coverage to use in simulations. PRA has tried to accommodate these requests, as the size of some of

CLDSIM's databases attests. However, the number of sources that collect and archive such data is limited. NOAA data at 1.1 km resolution is available, and PRA has routinely interpolated such data down to finer resolutions. The interpolation process was questioned during the BASS study (Albright, 1992). The point made was that validation needed to be done to determine the range of sizes over which scale invariance holds. At some scale, edge structure might be encountered that would produce higher clutter signals than predicted by the PSD-continuation method. Alternatively, highly correlated features might appear that would produce less clutter at small scales than scale invariance predicts.

To avoid doing this interpolation, PRA has acquired 30m resolution data from LandSat, although this is not a perfect solution either. Besides the cost involved in acquiring such data, there is the intrinsic problem that LandSat sensors are designed to image land features. In LandSat's analogue-to-digital conversion of the measured radiance, few bits are allocated to the radiance range associated with clouds, thus reducing the accuracy of the cloud data. PRA is also investigating acquiring aircraft data from NASA's ER-2 to provide high resolution data.

Although high resolution data should be used where possible, cost and availability considerations still leave a place for generating realistic, fine resolution databases from coarse data. Therefore, it is recommended that the PRA interpolation scheme be validated using high resolution databases that have been resampled to lower resolution and then interpolated to finer resolution again. PRA has pointed out that using scale invariance is equivalent to assuming that cloud structure is fractal in nature over a certain range. The fractal dimension of the structure in a cloud database can be related to the slope of the PSD used to generate it. A comparison of CLDSIM database fractal dimensions to the range of dimensions reported in the cloud literature would be useful. In general, Fourier techniques have difficulty generating realistic cloud structure because the information needed to produce the sharp edges seen in clouds is represented in the Fourier domain by complex relationships between the phases of the Fourier components. It is believed that PRA's interpolation method avoids this problem by using phases generated from the elliptical fits and by only altering the magnitudes of the components during the filtering process. Nevertheless, other methods of interpolation that do not require Fourier transforms, such as wavelets or traditional fractal techniques, might be investigated. If scaling laws for features of various sizes can be developed and validated, these techniques might be used to generate synthetic cloud altitude maps. This would provide a greater variety of cloud realizations to CLDSIM.

The question of the span of the conditions represented by the databases is tied to how they came into being. Historically, the databases have been produced at the request of one or more project offices wishing to simulate certain scenarios. Thus, there is a high concentration of cloud databases over the former Soviet Union. In selecting data sets to process, PRA looks at the archived data for the region of interest and chooses cloud conditions that are representative of stressing conditions. Measured against the clouds in the given region, the databases in CLDSIM are typical. The databases developed for specific projects become available to the general defense community through the SSGM, which raises the more general question of whether the set of CLDSIM databases span the range of clouds one could encounter for all scenarios. This is a difficult question to answer, largely because one needs to develop a log of cloud returns observed by sensors over a long period of time. The BASS study concluded that DSP data should be obtained to develop such a log. Until this can be done, PRA has worked to improve the coverage of databases by picking new geographic locations and cloud types to include. In the last year, the number of SSGM databases has grown from 10 to 17, with a mix of clouds from all latitudes.

A few general comments can also be made about the limitations of PRA's method of acquiring altitude databases. To obtain good IR images for cloud altitude maps, PRA selects NOAA data with high observer and solar elevation angles to minimize shadowing. (NOAA-9, used for the BSTS measurements, has local equatorial crossing times of 2:30 and 14:30.) This high elevation geometry emphasizes structural details of the top surface of the cloud over that of the cloud sides. This is not much of a problem if CLDSIM is used to simulate images of high altitude surveillance sensors in orbits similar to NOAA satellites, or if it is modeling cloud types with little vertical development. However, CLDSIM probably would have trouble modeling a thunderhead viewed from low elevation angles just using information obtained from high elevation data. In addition, if an optically thick cloud lies above another cloud, it is difficult to determine the surface features of the lower cloud using high elevation geometries. It is recommended that, if such data can be located, using stereoscopic measurements of cloud surfaces be considered to supplement current cloud altitude processing techniques. The proposed RAMOS experiment would provide such data.

When comparing CLDSIM to NOAA SWIR data, Mertz (1991b) pointed out that, besides surface variation effects, clutter in SWIR cloud radiances comes from variations in liquid water content (LWC) across the cloud. He proposed adding measures of the LWC obtained from water absorption bands as a way to increase cloud structure, especially for stratus clouds which may have rather smooth tops. While this might be a worthwhile addition to the model, CLDSIM would have to change its method of handling BRDFs to allow them to vary

with water content. The methods developed in Section 3 serve as one model for how this can be done.

Planned PRA Improvements to the Cloud Databases

PRA will continue to add more moderate resolution (30-120 m) databases for future releases of the SSGM. One new database is scheduled for the SSGM Release 6.0 in April of 1994, with perhaps 4-8 more available in late in 1994 or 1995. PRA is investigating using ER-2 aircraft measurements to improve spatial resolution.

PRA is developing global scale databases that will be run with simplifications of the CLDSIM model. For instance, diffuse scattering will be used, rather than relying on BRDFs. These databases are useful for scenarios with long flyouts or for geosynchronous observations of the earth. For Release 6.0, a database with 25-50 km resolution will be provided, while four more databases at 4 km resolution will be developed for future releases.

2.2 BRDFs

Besides the cloud altitude and type databases, CLDSIM requires precomputed tables of Bidirectional Reflectance Distribution Functions (BRDFs). A BRDF ρ_{BD} is defined in the following way: Let $H_i(\theta_i)$ be the irradiance at one wavelength incident on a surface, and let $L_r(\theta_r,\phi)$ represent the reflected radiance. Here the θ's are zenith angles measured with respect to the surface normal and ϕ is the azimuth angle between the incoming and outgoing radiation. Then $L_r(\theta_r,\phi)$ is given by

$$L_r(\theta_r,\phi) = \rho_{BD}(\theta_i,\theta_r,\phi)\ [H_i(\theta_i)\cos(\theta_i)]\ \cos(\theta_r) \qquad (1)$$

If H_r is the irradiance reflected into 2π, the directional reflectance, P_D is defined by

$$H_r = \rho_D(\theta_i)\ [H_i(\theta_i)\cos(\theta_i)] \qquad (2)$$

This gives

$$\rho_D(\theta_i) = \int_{2\pi} \rho_{BD}(\theta_i, \theta_r, \phi) \cos(\theta_r) \, d\Omega_r \qquad (3)$$

BRDFs are calculated for CLDSIM using the Multiple Scattering and Radiation Transport code, MSRAT. This routine computes the BRDF of a horizontally homogeneous cloud of a specified thickness, using an adding and doubling method. This method divides a region into small layers, each thin enough so that only single scattering is important. Upward and downward going fluxes for these layers are computed, and successively larger layers are constructed by combining sublayers, until the fluxes for the whole cloud are determined. The single scattering properties of the sublayers are computed using Mie theory, which assumes scattering by a distribution of spherical droplets of ice or water. Absorption of radiation inside the cloud by gaseous species is included by fitting the transmission as a function of centimeters of percipitable water vapor,

Table 2 - Precomputed MSRAT BRDFs

Database	**Cloud Type**
alto4.db	water
alto6.db	water
cumulo.db	ice above water
cirrus.db	ice
BRDF Variable	**Range**
Incident Zenith Angle	4 angles : 0, 30 ,60 ,80°
Reflected Zenith Angle	5 angles : 20, 45, 60, 72.5, 84.3°
Azimuth	9 angles : 0, 30, 50, 70 90, 110, 130, 150, 180°
Wavelength	50 values, 1 - 12.5 mm, variable resolution

y, to a series of exponentials (Stephens, 1978).

$$\tau(y) = \sum_{n=1}^{N} p(k_n) e^{-k_n y}; \quad \sum_{n=1}^{N} p(k_n) = 1 \qquad (4)$$

This allows one to handle gaseous absorption in the adding and doubling method by

adjusting the optical depths and single scattering albedo of each of the sublayers to include the optical depth due to one of the k_n. The BRDF is calculated for each n, and then averaged to give

$$\rho_{BD}(\theta_i, \theta_r, \phi) = \sum_{n=1}^{N} p(k_n)\, \rho_n(\theta_i, \theta_r, \phi) \qquad (5)$$

The four precomputed BRDF databases that are supplied with the SSGM are listed in Table 2. The BRDFs are computed for specific wavelengths, incident angles and reflected angles, which are also given in the table. Along with the BRDF values, the databases contain values of the cloud extinction, directional reflectance and directional emissivity as a function of wavelength.

Mie theory assumes spherical scatterers. This is a good model to use for water droplets, but does not adequately represent scattering from ice in cirrus clouds. There, ice platelets align horizontally due to hydrodynamic forces and can produce large specular returns. To handle this situation, CLDSIM uses a specular scattering model (Shanks, 1991). The model assumes a gamma distribution of ice particle volumes and uses empirical relations to compute their area. Geometric optics calculations are done to determine the expected reflected flux for a given set of incident and reflected angles. Due to statistical variations from perfect allignment, this flux is spread out over a lobe of a few degrees FWHM. The size and shape of this lobe comes from a model that takes as input the surface roughness and the correlation length of the particle misalignment. The SPCTBL routine is installed in the SSGM to allow computations of BRDFs with this model. Due to the great computation time involved, two precomputed databases are also supplied, one for a SWIR band and another for a band in the MWIR. These databases give a band-specific BRDF as a function of scattering angles and optical depth. In the SSGM implementation of CLDSIM, the user may choose whether or not to use the specular model. If chosen, it is applied to those cloud databases which contain cirrus clouds. The top 10% of the cirrus cloud is assumed to contain oriented ice crystals, while the bottom 90% contains spherical ice scatterers.

Critique of the MSRAT BRDFs

PRA has validated these calculations by comparing the BRDFs generated to a Monte Carlo BRDF calculation, to other adding and doubling calculations, and to experimental data. (See, for instance, Blasband and Jafolla, 1990.) A major focus of the present CLDSIM review has been on investigating CLDSIM's BRDFs. In Section 3, another approach to BRDF calculations is presented and compared to the CLDSIM BRDFs. In Section 4, differences

between CLDSIM results and measured radiances are attributed to the absence of correlated line transmission between the cloud scattering volume and the surrounding atmosphere.

Detailed discussion of the BRDFs will be taken up in those later sections. For now, a few general comments will suffice. First, although the MSRAT code can produce BRDFs for clouds of varying optical thickness, the BRDFs delivered in the SSGM correspond to optically thick clouds. As will be shown later, BRDFs of such clouds tend to have rather smooth variations as a function of angle, while BRDFs for thinner clouds contain peaks corresponding to glory scattering (180° backscatter) and rainbows (at about 140° backscatter). These are remnants of the phase function used for single scattering and tend to produce more contrast in cloud scenes.

To account for the drop in reflected radiance in thin clouds due to incomplete scattering, CLDSIM modulates its BRDFs by the cloud opacity, rather than calculating a new BRDF for each pixel. If τ is the cloud optical thickness, then the PRA technique uses

$$\rho_{BD}(\tau) = (1-e^{-\tau})\,\rho_{BD} \qquad (6)$$

While this technique accounts for a drop in reflected flux, it does not reproduce peaks in the BRDF seen in thin clouds when CLDSIM's starting BRDF corresponds to an optically thick cloud. A simple fix to this problem would be to interpolate smoothly between the single scattering solution and a large thickness solution as a function of optical depth. The single scattering solution for a given optical depth, $S(\tau)$, is a simple analytic expression that is developed in Section 3. Using this method, the correction for finite optical depth would be

$$\rho_{BD}(\tau) = [\rho_{BD}(\tau_{Large}) - S(\tau_{Large})]\,(1-e^{-\tau}) + S(\tau) \qquad (7)$$

Section 3 also presents a method of quickly computing BRDFs for various optical depths which goes beyond the single scattering technique. If either method of improving the thin cloud BRDFs is employed, the angular resolution of BRDFs will need to be finer than presently available in CLDSIM.

CLDSIM's BRDFs can also be evaluated in terms of variety. The SSGM is supplied with four BRDFs which represent a cirrus cloud, a cumulonimbus cloud, an altostratus cloud between 4 and 4.5 km altitude, and an altostratus cloud between 6 and 6.5 km. When the actual values of the BRDFs are compared, one finds that the two water cloud BRDFs are very similar, as are the cirrus.db and cumulo.db. As a sample of the BRDFs, the 0° solar

angle directional reflectances, $\rho_D(0)$ are plotted in Figs. 1 and 2. Note that equation 3 implies that the ϱ_D are averages of the BRDFs over reflected angles. Examination of these figures shows that the cirrus.db and cumulo.db values are essentially identical in these important sensor bands, although they do diverge from each other below 2.5 μm. The two alto databases show more variation, especially in the 4.35 to 4.5 μm region. This is due to an increase in gaseous absorption in the lower cloud relative to the higher cloud. However, if one looks at Table 1, one sees that the alto4.db is only used in the BALTIC database. Thus, in these two regions, one is largely left with two available BRDFs, one for a water cloud and another for an ice cloud.

The similarity of the BRDFs reflects the fact that they were created for optically thick clouds, where the effects of particle microphysics is minimal. The number of available BRDFs should increase to more accurately model thinner clouds. However, a difficulty in having more cloud BRDFs is that, if one is going to differentiate cloud types more closely, the process of typing the cloud altitude databases will become much more difficult. One possible solution is to allow the user to apply several different BRDFs to, say, a water cloud currently typed as alto.

Planned PRA Improvements to the BRDFs

The present BRDFs in CLDSIM are being recalculated for the April 1994 Release 6.0 of the SSGM to extend the spectral range from 1-12.5 μm to .2 - 15 μm. The resolution from 2.6 -3.0 μm will go from .04 mm to .01 mm. These BRDFs will have adjustments to their microphysical parameters. In addition, the angular resolution of the BRDFs will change from 4 solar zenith angles to 12, from 5 observer angles to 15, and from 9 azimuth angles to 27. For Release 7.0 in late 1994, two new BRDFs are also planned. These may be a thin cirrus cloud and a stratocumulus cloud.

2.3 Steps in the CLDSIM Calculation

When CLDSIM is run in the SSGM, a series of separate programs are executed in succession. The major ones are APART, which produces input radiances and fluxes on a fine spectral scale; ATCALC, which converts these to inband quantities; and CLDSIM, which produces radiances. CLDSIM itself is divided into CLDTPO, CLDGEO, CLDRAD and FOOTPR, which determine the cloud top normals, calculate scattering angles, put together the pieces that form the radiance for each cloud pixel, and footprint the pixel radiances for the viewer's perspective. These functions will be described below.

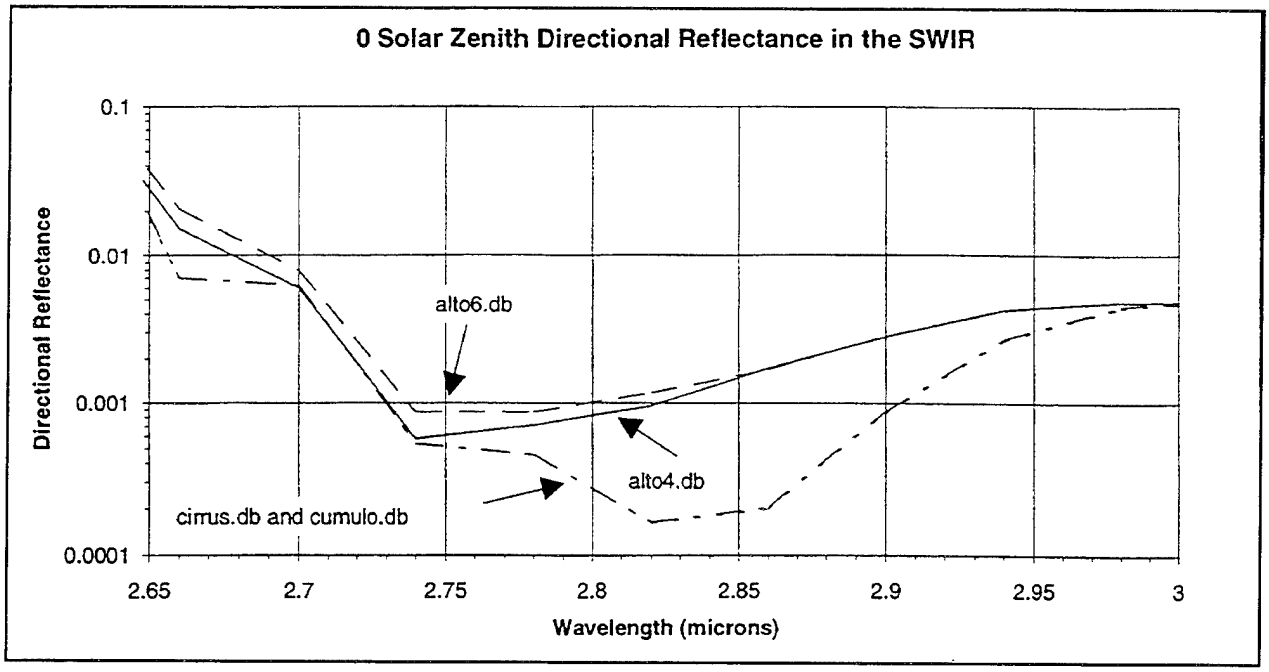

Figure 1. Directional reflectance in the SWIR

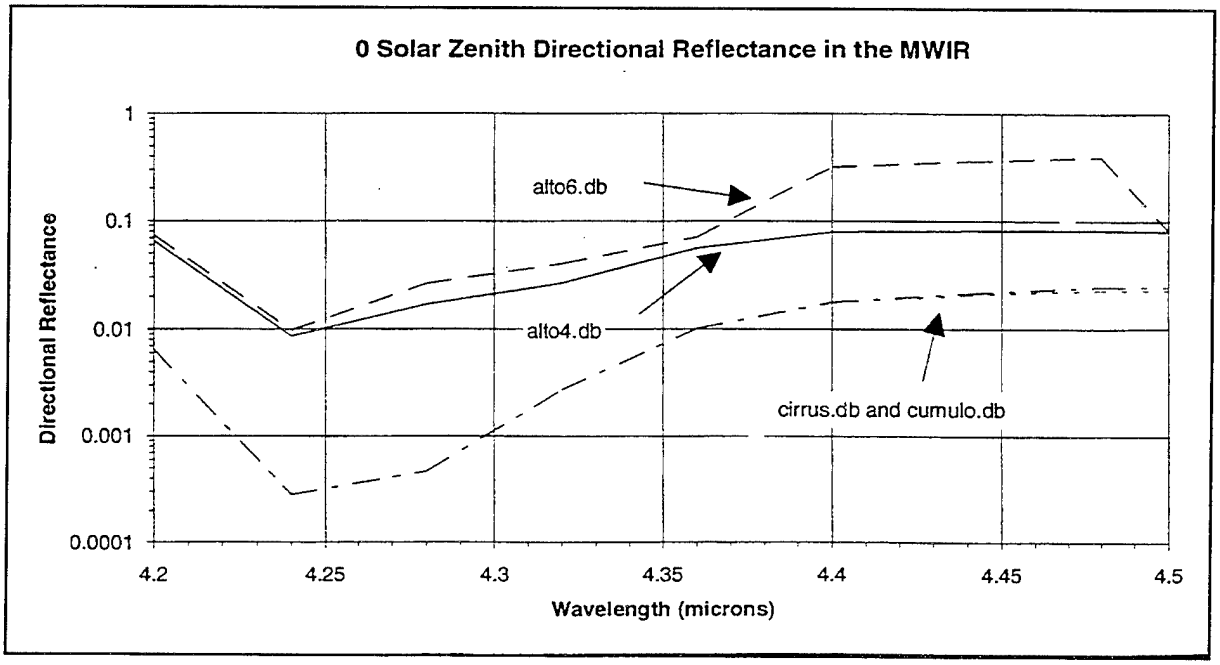

Figure 2. Directional reflectance in the MWIR

Table 3 is useful in describing the variables encountered.

A user wishing to run CLDSIM in the SSGM begins by setting up a Scenario Definition File (SDF). This file gives the input choices to the user. They include

(1) the date and time of day (to fix the solar position);
(2) the observer position;
(3) the wavelength limits of the sensor, or a file giving its spectral response;
(4) the IFOV and number of pixels in the output scene;
(5) the cloud altitude database desired;
(6) the latitude and longitude of the altitude database (to locate it on the earth);
(7) the atmospheric profile (temperature and pressure as a function of altitude) from a list of profiles;
(8) the type of terrain background to put below the clouds.

Other switches are also available to do such things as turn on or off the specular BRDF for cirrus clouds, or to produce diagnostic plots that identify the cloud type below each pixel.

The SSGM takes this information and prepares input decks for the various codes. It first calls APART, which supplies temperature, transmission, solar irradiance, thermal and solar skyshine, and thermal and solar path radiance. These quantities are defined for eleven altitudes, from 0 to 10 km, and at a high spectral resolution. The inputs to this routine are the model atmosphere (from a list of 23 choices) and the solar and observer positions. For purposes of interpolation, APART is run twice, each time using one of two solar zenith angles that bound the range of solar positions that exist at different parts of the cloud database. This allows the solar angle to vary across the cloud. In addition, the observer zenith angles at the four corners of the cloud database are used to bound the observer angle, with interpolation for this variable occuring inside the cloud. It should be noted that when a time series of cloud images is requested (a "movie" to use the SSGM term), the solar and observer positions are fixed to be that of the center time for the time series. Thus, the sun and observer do not move over the time interval. Rather, the final output is simply foot printed into the correct viewer position for each time.

APART is based on LOWTRAN and provides radiant quantities at 5 cm^{-1} resolution. Inband quantities are required for the final output. The SSGM calls ATCALC to integrate APART output over a spectral band, using a user-specified spectral response function if desired. ATCALC also takes the temperature information from the APART output to create

Table 3. Quantities used in CLDSIM

Variable	Description
θ_{sol} , θ_{obs} , ϕ	Solar Zenith Angle, Observer Zenith Angle, Azimuth, measured relative to the local vertical
θ'_{sol} , θ'_{obs} , ϕ'	Solar Zenith Angle, Observer Zenith Angle, Azimuth, measured relative to the cloud surface normal
z	Altitude
λ	Wavelength (or band of wavelengths)
T(z)	Temperature at altitude z
$\tau(\lambda,z)$	Transmission from altitude z to the observer
$\chi(\lambda)$	Cloud extinction (per km of cloud)
Op $(z-z_{bot}, \theta)$	Cloud opacity (with z_{bot} the altitude of the cloud bottom)
P_D (θ_{sol}, λ)	Directional reflectance of the cloud
ϵ (θ_{sol}, λ)	Directional emissivity of the cloud
$P_{BD}(\theta'_{sol}, \theta'_{obs}, \phi', \lambda)$	Cloud Bidirectional Reflectance Distribution Function (BRDF)
ϵ_{grnd} (λ)	Emissivity of the ground
H_{sol} $(\theta_{sol}, \theta_{obs}, \lambda, z)$	Solar irradiance
L_{bb} $(\theta_{sol}, \theta_{obs}, \lambda, T(z))$	Blackbody radiance determined by the local temperature
L_{pt} $(\theta_{sol}, \theta_{obs}, \lambda, z)$	Thermal path radiance
L_{ps} $(\theta_{sol}, \theta_{obs}, \lambda, z)$	Solar path radiance
L_{st} $(\theta_{sol}, \theta_{obs}, \lambda, z)$	Thermal skyshine radiance
L_{ss} $(\theta_{sol}, \theta_{obs}, \lambda, z)$	Solar skyshine radiance

tables of inband blackbody radiance at the 11 altitudes. It merges the radiance information from APART with the BRDFs to produce the input files necessary to run CLDSIM itself.

When CLDSIM is invoked, the code first runs its CLDTPO routine. CLDTPO determines the normal to the cloud surface at each pixel by fitting a plane through the four surrounding points. Special attention is given to cloud edges which don't have all four surrounding pixels covered by clouds of the same type. When CLDTPO finishes, it writes out a file four times larger than the original cloud altitude database. It contains the cloud altitude and the three components of the surface normal for each pixel.

CLDSIM next calls CLDGEO, which uses the observer and solar position (at the center time of a time series) to calculate the solar zenith angle, observer zenith angle and the azimuth angle between the sun and the observer for each pixel. Two sets of angles are computed. The first, θ_{sol}, θ_{obs}, and ϕ, are measured relative to the local vertical, with the second, θ'_{sol}, θ'_{obs} , and ϕ', are measured relative to the surface normal. The latter set is used for solar scattering. CLDGEO ends after creating a file that contains the cosines of these six angles listed for each pixel.

CLDRAD is next called by CLDSIM to calculate the radiance for each pixel. Inputs are the ATCALC output file, the cloud altitude file, and the file containing the six cosines for each pixel. The routine loops over pixels and performs the necessary interpolations on the radiant quantities. Most quantities must be interpolated over the solar and observer zenith angles (measured relative to the local vertical), as well as the altitude. The BRDF must be interpolated over the two zenith angles and azimuth angle that are measured with respect to the surface normal. All interpolations are done on the logarithm of the radiance. The radiant quantities are combined in one of several ways, depending on angular conditions. If the surface normal is not directed toward the observer ($\theta'_{obs} > 90°$), the pixel is assumed to be in a shadow, and no radiance is returned. In addition, if the solar zenith θ_{sol} is greater than 90°, "night time" calculations are performed for the pixel. This involves turning off solar scattering and, if the sun is below a user selected angle, the solar path radiance. For night, the equation used by CLDRAD is

$$
\begin{aligned}
L \;=\; & [\epsilon * \tau * L_{bb} * Op] && : \textit{cloud blackbody} \\
& + [\rho_D * (L_{ss} + L_{st})] && : \textit{solar + thermal skyshine} \\
& + L_{pt} * Op && : \textit{thermal path radiance} \\
& + L_{bkg} * (1 - Op) && : \textit{background radiance}
\end{aligned}
\qquad (8)
$$

while for "daytime" conditions, CLDRAD uses

$$
\begin{aligned}
L \;=& (H_{sol}*\cos(\theta'_{sol}))\rho_{BD}*Op && : \textit{reflected solar radiance} \\
&+(H_{sol}*\cos(\theta_{sol}))\rho_{D}*Op*(\rho_{D}/24) && : \textit{diffuse solar radiance} \\
&+[\epsilon*\tau*L_{bb}*Op]*(1+\rho_{D}/24) && : \textit{cloud blackbody} \\
&+[\rho_{D}*(L_{ss}+L_{st})]*(1+\rho_{D}/24) && : \textit{solar + thermal skyshine} \\
&+[L_{ps}+L_{pt}]*Op && : \textit{solar + thermal path radiance} \\
&+L_{bkg}*(1-Op) && : \textit{background radiance}
\end{aligned}
\qquad (9)
$$

A few quantities in these expressions deserve further explanation. The opacity, Op, is obtained using the cloud extinction contained in the BRDF datafile, multiplied by the vertical distance between the cloud top and cloud bottom. It is used to adjust the cloud radiance for

$$Op = 1 - e^{-\chi\,(z - z_{bot})} \qquad (10)$$

small optical depth. The terms proportional to $P_D/24$ approximate the diffuse radiance from the cloud's environment. The background radiance, L_{bkg}, represents the radiance of the underlying terrain. It can come from a file containing radiances calculated using PRA's GENESSIS model, or it can be determined from a statistical description of the reflectance of the ground. From a user-supplied pair of mean reflectance and variance values, CLDRAD can calculate a random emissivity for each pixel, and determine the radiance for "night time" conditions using the equation

$$
\begin{aligned}
L_{bkg} \;=& L_{bb}*\tau*\epsilon_{grnd} && : \textit{ground blackbody radiation} \\
&+L_{pt} && : \textit{thermal path radiance}
\end{aligned}
\qquad (11)
$$

For daylight conditions, the equation is

$$
\begin{aligned}
L_{bkg} \;=& L_{bb}*\tau*\epsilon_{grnd} && : \textit{ground blackbody radiation} \\
&+H_{sol}*\cos(\theta_{sol})*(1-\epsilon_{grnd}) && : \textit{reflected sunlight} \\
&+(L_{ps}+L_{pt}) && : \textit{solar+thermal path radiance}
\end{aligned}
\qquad (12)
$$

All of these quantities refer to ground conditions with z = 0.

The final call to a major CLDSIM routine is to FOOTPR, which transforms the cloud scene from a pixelization based on the altitude database to one based on the sensor IFOV. This

routine assumes that the cloud database is a portion of a cylinder curving away from the viewer. This allows for foreshortening effects, but does not accurately represent the curvature of the earth in the azimuth direction. Following the FOOTPR call, the output radiance scene is composited with other scene elements in the SSGM.

In discussing the steps used to produce a CLDSIM image, several details have been omitted. For instance, a cloud transmission file can be created from the computed opacity values. This file can be used to obscure objects below the cloud. Further, CLDSIM can be run with the HORIZON code to produce a scene with clouds merging with the earthlimb. Special techniques are used to match radiances at the horizon, but they will not be treated here.

PRA's Validation of CLDSIM

PRA has performed several studies to validate parts of CLDSIM. Blasband and Jafolla (1990) compare predicted radiance values spectrally across the 2.6-3.0 μm band to A.D. Little data obtained from aircraft measurements. This served as a test of the BRDFs and radiance equations, but did not test the processes used to construct a cloud altitude map. Averaged over the spectral band, the CLDSIM radiance was within a factor of 2 to 4 of the A.D. Little data, but it showed considerable differences when one examined the spectrum. CLDSIM had trouble reproducing either the peak in radiance from about 2.65-2.8 μm, or the region outside this band. Section 4.0 discusses a possible reason for this.

One difficulty using the A.D. Little data was that little information was available to PRA about the properties of the specific clouds observed. This problem was ameliorated when PRA tested CLDSIM and the altitude database generation process using NOAA data (Mertz, 1991b). Here NOAA AVHRR data was used to construct a database, and then CLDSIM was run to try to reproduce the data. Comparisons were done using bands at 0.86, 3.71, 10.74 and 11.86 μm. A standard BRDF was used because the microphysics of the cloud scatterers was not contained in the data. The accuracy of CLDSIM was gauged using the mean, standard deviation, and extrema of the predicted radiances, as well as the correlation coefficient between the data and the simulated scenes. For the two LWIR bands the agreement was excellent, with correlation coefficients above 99%. This was expected since these bands were used to construct the database. For the two bands which contained solar scattering, the agreement was good, but the correlation coefficients dropped to around 50%. This was attributed to too much contrast being produced by CLDSIM when it turned on and off pixels depending on their orientation to the sun and observer.

At the same time, CLDSIM was also tested against the absorption band data from HIRS/2, which is part of the TOVS data product used to determine the atmospheric profile for database generation. Agreement here was good, although in strongly absorbing bands where one has trouble seeing to the cloud layer, CLDSIM did not reproduce the exact structure in the observed data, even though it did correctly predict a low variance. This is due to the fact that, in CLDSIM, structure comes from cloud top variations, and structure in the atmosphere above the clouds is not modeled.

To test CLDSIM in the SWIR and to validate the specular model, PRA collected DSP returns near a specular scattering geometry (Shanks, 1992a). Coincident GOES and AVHRR data were also collected. The AVHRR data was used to construct the BAJA database. CLDSIM was executed using this database, and its predicted radiances were then run through PRA's model of the DSP sensor. When the specular model was turned on, the exceedance plot obtained from the model compared well with the data for large intensities. For lower intensities, DSP's complex processing techniques made comparison difficult. When one compared the spatial distribution of returns between the real and simulated data, one found significant differences. The DSP returns were much more concentrated than the CLDSIM returns.

During the BASS study, a further comparison was done between CLDSIM and DSP data (Albright, 1992). This comparison was not a validation of CLDSIM, but it was an attempt to compare the distribution of clutter computed using a standard CLDSIM database with that observed by an operational system. Similar viewing geometries were used, but no attempt was made to match cloud type, altitude, cover amount, or microphysics. Further, the DSP data sets were only claimed to be representative on the basis of anecdotal evidence. Comparisons were done for a specular geometry, a geometry near specular and a diffuse geometry. Exceedance plots showed that CLDSIM predicted more severe returns for its database in the specular geometry than the data showed, while underpredicting the returns for the diffuse geometry. These results may be affected by two factors. First, the CLDSIM scene was generated with an unphysical arctic atmosphere over equatorial clouds to enhance clutter. Second, PRA subsequently discovered a bug in the MSRAT code's treatment of gaseous absorption, which has the effect of underestimating mean cloud radiance by a few percent up to 80% depending on altitude and geometry.

The specific details of the BASS CLDSIM / DSP comparison limits its usefulness for making general statements about CLDSIM. Still, comparison of standard CLDSIM images to statistically significant sets of operational data is an important complement to the cloud-

matched NOAA and PRA DSP validation efforts reported above. Such a comparison is needed to let the system developer know how many CLDSIM images must be analyzed to represent the range of expected returns for a given scenario, and to guide PRA in expanding the set of cloud altitude databases. A start along these lines is represented by a study PRA performed using CLDSIM to predict the range of returns a BP constellation would observe over a year (Shanks, 1992b). This study provides context so that the clutter from an individual CLDSIM scene can be compared to the range of clutter produced by CLDSIM. A similar study could be done for the DSP sensor or for MSX, so that range of CLDSIM returns could be compared to statistics from large numbers of measurements from these instruments.

Critique of CLDSIM Calculational Steps

The previous CLDSIM validation has shown that CLDSIM produces reasonable radiance values for many conditions. However, a few improvements can still be suggested.

The CLDSIM methods for handling cloud illumination and shadowing are local in nature. A pixel is illuminated or not depending on its orientation with respect to the sun and the viewer. Thus, a pixel facing the sun but hidden from it by an intervening cloud mass is treated as if the mass is not there. Similarly, pixels receive the same diffuse radiation contribution whether they are illuminated by surrounding clouds or face into space. This local handling of shadowing and illumination is a reasonable approximation for high elevation angle geometries where cloud-on-cloud interactions are slight, but becomes less reasonable at lower elevation angles. It is recommended that shadowing and cloud-on-cloud illumination be improved to handle non-local effects. This might be done by generating coarse resolution representations of the cloud top surface to determine line-of-sight intersections with the cloud, and finer resolution data to determine the fine structure of scattering.

CLDSIM treats scattering as a surface effect, while scattering actually takes place throughout a volume. The calculations of CLDSIM's BRDFs take this fact into account by computing multiple scattering throughout an infinitely thick slab. As long as the radius of curvature of the cloud surface is large compared to the mean free path between scatters, this geometry is accurate. However, closer range TMD sensors may look at clouds in finer detail and at lower elevation angles, and observe structures with small radii of curvature. The protrusions on cumulus clouds serve as good examples. In that case, using BRDFs computed for spherical scattering volumes may be more accurate than the slab BRDFs.

Two - perhaps offsetting - approximations affect the accuracy of CLDSIM's treatment of background radiation from the terrain below the cloud. When CLDSIM includes background radiation, it attenuates it using beam transmission equations. Thus, L_{bkg} is multiplied by (1-Op) which is exp (-c (z-z_{bot})). This factor represents the fraction of the upwelling radiance that is neither scattered nor absorbed as it passes through the cloud. However, much of the scattered radiance is scattered in the forward direction and passes through the cloud. The beam transmission equation misses this radiance, and so underestimates the contribution of L_{bkg} to the final radiance. Simple changes to the beam transmission equation could approximate the scattering contribution. Using ideas developed in Section 3, the change needed is

$$\chi \rightarrow \chi' = \chi \ (1-\omega_0 f) \qquad (13)$$

Here f is a measure of the fraction of light scattered in the forward direction.

Offsetting the increase in L_{bkg}'s contribution obtained if the suggested approximation is used is the fact that as the radiance travels through the cloud it is spread out. Thus, the sharpness of clutter below the cloud is reduced by passing through the cloud. This reduces the effect of background clutter. It is not known which effect predominates: the forward scattering that increases the transmitted terrain clutter or the spreading of the beam that washes it out.

As mentioned before in discussing PRA's validation of CLDSIM against NOAA data (Mertz, 1991b), CLDSIM produces unstructured scenes in highly absorbing bands which have neglible transmission down to the cloud layer. To remedy this situation, PRA should include atmospheric gravity waves and other sources of atmospheric structure if they become available in atmospheric state codes.

Critique of CLDSIM in the SSGM

CLDSIM is a code that is typically run in one of two ways: it is run either as a stand-alone code by people experienced in atmospheric physics, or it is run by people of diverse training as part of the SSGM. There are significant differences between these two ways of running CLDSIM. When CLDSIM is run as a stand-alone code, it often uses cloud top altitude databases specifically constructed for a particular problem, while the general user of CLDSIM must use one of the seventeen pre-set databases. Very little information is provided in the SSGM about the meterology represented in the databases, and the range of conditions each

one is good for. The CLDSIM user is thus left wondering which clouds can legitimately be used in a particular scenario, and whether the databases in the SSGM span the likely cloud cover one could expect. In addition, there is minimal error checking in the SSGM to make sure that consistent sets of inputs are used. Such error checking is crucial to insure that time and money is not needlessly spent analyzing inaccurate results. In addition, any warnings that CLDSIM does give should be transmitted with the image, perhaps by placing them in the image's header. During the BASS study, this would have helped remind users that several of the images were clutter-enhanced due to a choice of an unphysical atmosphere profile. Increased error checking, warning messages, and on-line documentation are scheduled to be incorporated into future releases of the SSGM. Physically based input checks and on-line help for using cloud databases should be aggressively pursued for early inclusion in the SSGM.

Another feature that reduces CLDSIM's utility in the SSGM is its slow running time. Typical run times are 30 minutes to 2.5 hours on a SGI 4D-25 for a reasonably sized cloud image. CLDSIM has an architecture that causes it to compute facet normals or scattering angles for all pixels in a cloud altitude database, whether the pixels are to be part of the final image or not. Thus, it takes about the same time to generate a cloud image of a few dozen square kilometers as it does to make an image covering the region from Mexico to Alaska. CLDSIM is being rewritten to meet new timing requirements, and a feature is being added to allow one to cut out a small region of interest from a large cloud database before processing begins. A reorganization of data in CLDSIM is also being planned. While it is impossible to judge the time savings these changes will make before they are fully implemented, if significant time savings occur, they will make CLDSIM a much more valuable tool. When scenes are relatively easy to produce, engineering studies of the variation of returns with solar position and atmospheric condition will be attractive to the general CLDSIM user.

Because CLDSIM has been slow in the past, PRA has implemented a zeroth-order method of allowing cloud images to change with time. A time series of cloud images are calculated assuming the solar and observer positions are fixed in time. Thus, temporal variations in cloud scenes come from changes in the observer position that is given to footprinting routines, rather than changes in the angles used in the radiance calculating routine CLDRAD. To see what effect this approximation has on a simulation, Visidyne ran a case with specular scattering off of the BAJA databases at low elevation angles (25°). The specular scattering model was used because of the narrow peak of the BRDF in this model. Parameters were chosen to approximate a BE-like sensor. Scenes were generated two per

second for a time sequence of 10 seconds using the single-time approximation. Then two consecutive frames were reproduced using separate SSGM runs. Consecutive frames were differenced, and the two difference images - one from the time series and the other from separate runs - were compared, both visually and using their exceedance plots. Because of the over 2000 km range between the sensor and the cloud, and the fast frame rate, no significant difference was observed between the two methods of calculating the scenes. Although a simple time interpolation method probably should be added to CLDSIM, and doing so would not be very difficult, this single test case does not provide compelling evidence that it is necessary.

Planned PRA Improvements to CLDSIM

CLDSIM is being extensively rewritten for Release 6.0 of the SSGM (due April 1994). The input files to CLDSIM are being reorganized to group data differently, and the code is being streamlined for speed. The ability to select just a section of a large altitude database for processing will be added through CLDSIM "cookie cutter" capability. Also, a capability will be added to allow the user to tile a region with replicas of a single cloud database to cover cases such as observing a long missile fly-out with a small FOV.

A major goal for Release 7.0 (late 1994) is to replace pixels in the cloud databases with triangular facets, which are easier for SGI hardware to handle. Transforming from pixels to facets will allow the user to vary the resolution of the database for increased throughput. For instance, high resolution sections of the database could be placed around regions of interest in a cloud scene (say near a target being tracked), while lower resolution representations could be used elsewhere.

The facet model will also be used to improve the cloud shadowing. Facets will be ordered by distance away from the sun, and facets with more than 50% of their area obscured by other facets will be in shadow. Facets will then be ordered by distance from the observer, and unobscured facets will be projected onto the final image. This does not seem to cover the issues of cloud-on-cloud illumination and backlighting of surfaces, but it is a start.

APART is to be replaced in Release 6.0 with the MOSART atmospheric transport code. A three-stream cloud-over-terrain model will be implemented which takes into account the exchange of radiation between these features. A three-stream cloud-over-cloud model will come in Release 7.0. In addition, the cylindrical geometry assumed in the present footprinting routines will be replaced by a full 3-D algorithm.

3. VISIDYNE CLOUD SCATTERING MODEL

In order to test the CLDSIM's BRDFs, Visidyne adapted the radiation transport code used by NORSE and its predecessors to compute BRDFs for various particle size distributions and cloud types (Ewing, 1978). The code consists of MIECODE, a Mie scattering routine to compute the phase function of a given particle distribution, and SLAB, a routine that approximates multiple scattering in a slab of given thickness. They are joined together in the program MSLAB. The routines are described in the next section, which is followed by reports on the validation of MSLAB and computations testing CLDSIM's BRDFs.

3.1 Description of MSLAB

Visidyne's MIECODE is a standard Mie code that calculates the phase function $p(\alpha)$, scattering coefficient k_s and absorption coefficient k_a for a distribution of spherical droplets. The inputs are the complex index of refraction at the wavelength of interest and parameters characterizing the droplet distribution. Although several distributions are available, MIECODE was modified to follow PRA's practice of representing the cloud droplet distribution as a modified gamma distribution defined over a range of radii between r_{min} and r_{max}. Throughout that range the number of drops per cubic centimeter with radius r is given by

$$n(r) = N_T A \left(\frac{r}{r_0}\right)^{\alpha-1} e^{-\left(\frac{r}{r_0}\right)^{\gamma}} \qquad (14)$$

Here N_T gives the total number of drops per cubic centimeter and A is a normalization constant that depends on r_{min} and r_{max}. If these are set to zero and infinity respectively, A is given by

$$A = \frac{\gamma}{r_0 \, \Gamma\left(\frac{\alpha}{\gamma}\right)} \qquad (15)$$

where Γ is the gamma function. The quantities r_0, α and γ determine the distribution's shape.

SLAB approximates multiple scattering in a slab of a given thickness using single scattering enhanced by estimates of the multiple scattering contribution. To see how this is done, let $L(s,\Omega)$ represent the radiance along a path at pathlength s, radiating in the direction

$$\frac{dL}{ds} = -k_e L + J \qquad (16)$$

W, where W can be described by the spherical coordinates θ and ϕ. As it propagates, the radiation suffers extinction governed by the coefficient k_e, and picks up radiance due to the scattering of light into the Ω direction, represented by the source term J. The radiation transport equation has the solution

$$L(s,\Omega) = L(s_0,\Omega)\, e^{-k_e(s-s_0)} + \int_{s_0}^{s} J_{ext}(s',\Omega)\, e^{-k_e(s'-s_0)}\, ds' \qquad (17)$$

where

$$J_{ext}(s',\Omega) = \frac{k_e \omega_0}{4\pi} \int_{4\pi} L_{ext}(s',\Omega')\, p(\Omega,\Omega')\, d\Omega' \qquad (18)$$

Consider light scattered off of a cloud top. Let z measure the distance down from the top of the cloud, which has a vertical thickness of l, and let s be at the cloud top, where z=0. Then

$$(s-s') = \frac{z}{\cos(\theta)} = \frac{z}{\mu};\ \mu = \cos(\theta) \qquad (19)$$

Let $L(\Omega) = L(0,\Omega)$ be the radiation coming out of the cloud in the Ω direction. Switching from s to z, and ignoring the upwelling background radiation contained in the $L(s_0,\Omega)$ term gives

$$L(\Omega) = \int_0^l J_{ext}(z,\Omega)\, e^{-\frac{k_e z}{\mu}} \frac{dz}{\mu} \qquad (20)$$

The $L_{ext}(s,\Omega')$ term in equation 3.1.5 contains light that has been multiply scattered, as well as single scattered light. The contribution to the cloud top radiance of single scattered light is easy to calculate. If the light at the top of the cloud comes in from the Ω_0 direction, the illuminating light at the top of the cloud is given by

$$L_0(0,\Omega') = I_0\, \delta(\cos(\theta') - \cos(\theta_0))\, \delta(\phi' - \phi_0) \qquad (21)$$

Applying the attenuation factor exp(- k_e z / μ') to get the amount of the illuminating radiation that does not scatter until reaching the z level, and integrating over Ω' gives

$$
\begin{aligned}
&J_{ss}(z,\Omega) \\
&= \frac{k_e\omega_0}{4\pi}\int p(\Omega,\Omega')\, I_0\,\delta(\cos(\theta')-\cos(\theta_0))\,\delta(\phi'-\phi_0)\, e^{-\frac{k_e z}{\mu'}}\, d\Omega' \\
&= \frac{k_e\omega_0}{4\pi} I_0 p(\alpha)\, e^{-\frac{k_e z}{\mu_0}}
\end{aligned}
\tag{22}
$$

Here α is the scattering angle between Ω and Ω'. The expression for the single scattered outgoing radiance is

$$
L_{ss}(\Omega) = \frac{\omega_0}{4\pi} I_0 p(\alpha)\, \frac{\mu_0}{\mu+\mu_0}\left(\, 1-e^{-k_e l \frac{\mu+\mu_0}{\mu\mu_0}}\,\right) \tag{23}
$$

To estimate the multiple scattering contribution, SLAB follows the NORSE code and defines a build-up factor B(z) that estimates the ratio of the multiply scattered radiation from the z level to the single scattered radiation. To define B, consider the fraction f_e of light single scattered at z that escapes out of either the cloud top or bottom without scattering again.

$$
f_e(z) = \frac{\int_{4\pi} J_{ss}(z,\Omega')\, e^{-\frac{k_e z}{\mu'}}\, d\Omega'}{\int_{4\pi} J_{ss}(z,\Omega')\, d\Omega'} \tag{24}
$$

For simple geometries, such as a slab geometry, f_e can be evaluated analytically.

Of the radiation first scattered at z, the fraction f_e escapes without further interactions, while the fraction $f_r = (1-f_e)$ either is absorbed or scattered. Since$_0\omega$ gives the ratio of scattering to extinction, the fraction $\omega_0 f_r$ of the light survives the second scattering without being absorbed, and the fraction $\omega_0 f_r f_e$ escapes the cloud. In the same way, the fraction of the light that escapes after scattering n times is $(\omega_0 f_r)^{n-1} f_e$. Summing up the contributions and dividing by the fraction escaping after only one scatter gives the build-up factor

$$
\begin{aligned}
B(z) &= \frac{1}{f_e}\sum_{n=1}^{\infty} f_e(\omega_0 f_r)^{n-1} \\
&= \frac{1}{(1-f_r\omega_0)} = \frac{1}{(1-(1-f_e)\omega_0)}
\end{aligned}
\tag{25}
$$

The amount of multiple scattered light can be estimated using the build-up factor. The next question to decide is how to include this light in the outgoing radiation. The Rayleigh scattering pattern holds for radiation scattered off of droplets small compared to the wavelength ($x = 2\pi r/\lambda << 1$) and is approximately isotropic. (Rayleigh scattering goes as $(1+\cos^2(\alpha))/2$, giving a factor of two variation.) Scattering from large droplets ($x >> 1$) has a pattern that is highly forward peaked. To determine how peaked the scattering is, the SLAB code uses the forward directivity integral of the Mie phase function, defined by

$$f = \frac{1}{2} \int_{-1}^{1} p(\alpha) \cos(\alpha) \, d\cos(\alpha) \qquad (26)$$

It then approximates the phase function by assuming that a fraction of the light given by f is scattered in the forward direction and that the rest of the light, (1-f), is scattered isotropically. In the interaction represented by equation 3.1.3, the extinction term $k_e L$ is the sum of the part $k_a L$ that is absorbed and the part $k_s L$ ($= \omega_0 k_e L$) that is scattered. SLAB assumes that the fraction f of scattered light is scattered precisely in the forward direction. This is handled mathematically by adding back on the right hand side of equation 3.1.3 the amount $k_s f L$.

$$\frac{dL}{ds} = -k_e L + J + k_s f L = -k_e (1 - \omega_0 f) L + J \qquad (27)$$

The effect of this is to replace the extinction coefficient k_e in the radiation transport equation with the quantity $k_e (1 - \omega_0 f)$.

With these approximations, NORSE calculates the cloud top radiance as a sum of single scattered and multiple scattered radiance

$$L(\Omega) = L_{ss}(\Omega) + L_{ms}(\Omega) \qquad (28)$$

where

$$L_{ss}(\Omega) = \frac{k_e \omega_0}{4\pi} \int_0^l \int_{4\pi} p(\Omega, \Omega') L_0(0, \Omega') e^{-\frac{k_e(1-\omega_0 f)z}{\mu'}} d\Omega' e^{-\frac{k_e(1-\omega_0 f)z}{\mu}} \frac{dz}{\mu} \quad (29)$$

and

$$L_{ms}(\Omega) = \frac{k_e \omega_0}{4\pi} \int_0^l \int_{4\pi} (B(z)-1)(1-f) L_0(0, \Omega') e^{-\frac{k_e(1-\omega_0 f)z}{\mu'}} d\Omega' e^{-\frac{k_e(1-\omega_0 f)z}{\mu}} \frac{dz}{\mu} \quad (30)$$

In the above, the term -1 occurs in the factor B-1 to remove single scattering from the multiple scattering factor and (1-f) is used to give the fraction of the scattered radiation that has not been assigned to the forward direction. The phase function for isotropic scattering is unity.

The Mie and SLAB codes are combined in the MSLAB routine to take as inputs cloud droplet distribution parameters and cloud altitudes, and to give as output BRDFs for chosen wavelengths and scattering geometries. CO_2 and H_20 gaseous absorption inside the cloud is handled using a weak line approximation. The amount of these gases is determined by computing the partial pressures of these gases in an atmosphere with a constant scale height and lapse rate. The water vapor is assumed to be at 100% relative humidity.

3.2 Validation of MSLAB BRDF Calculations

To gain confidence that the MSLAB code could accurately calculate BRDF's, several test cases were run. The tests include calculating

(1) the slab scattering BRDF using a simple phase function;
(2) the Mie theory phase function;
(3) BRDFs as a function of optical depth;
(4) BRDFs as a function of particle size; and
(5) BRDFs with and without gaseous absorption.

Slab Scattering

An exact multiple scattering solution has been calculated by Chandraskhar for the case of an infinitely thick slab and isotropic scattering. The MSLAB calculations for this case are plotted against his results in Figure 3. The results are plotted as the ratio of predicted scattering to Lambertian scattering for the same single scattering albedo, ω_0. The results show that MSLAB does fairly well in reproducing the exact solution. It has the greatest difficulty for radiation traveling along the slab surface (at a zenith angle of 90°), for high scattering conditions.

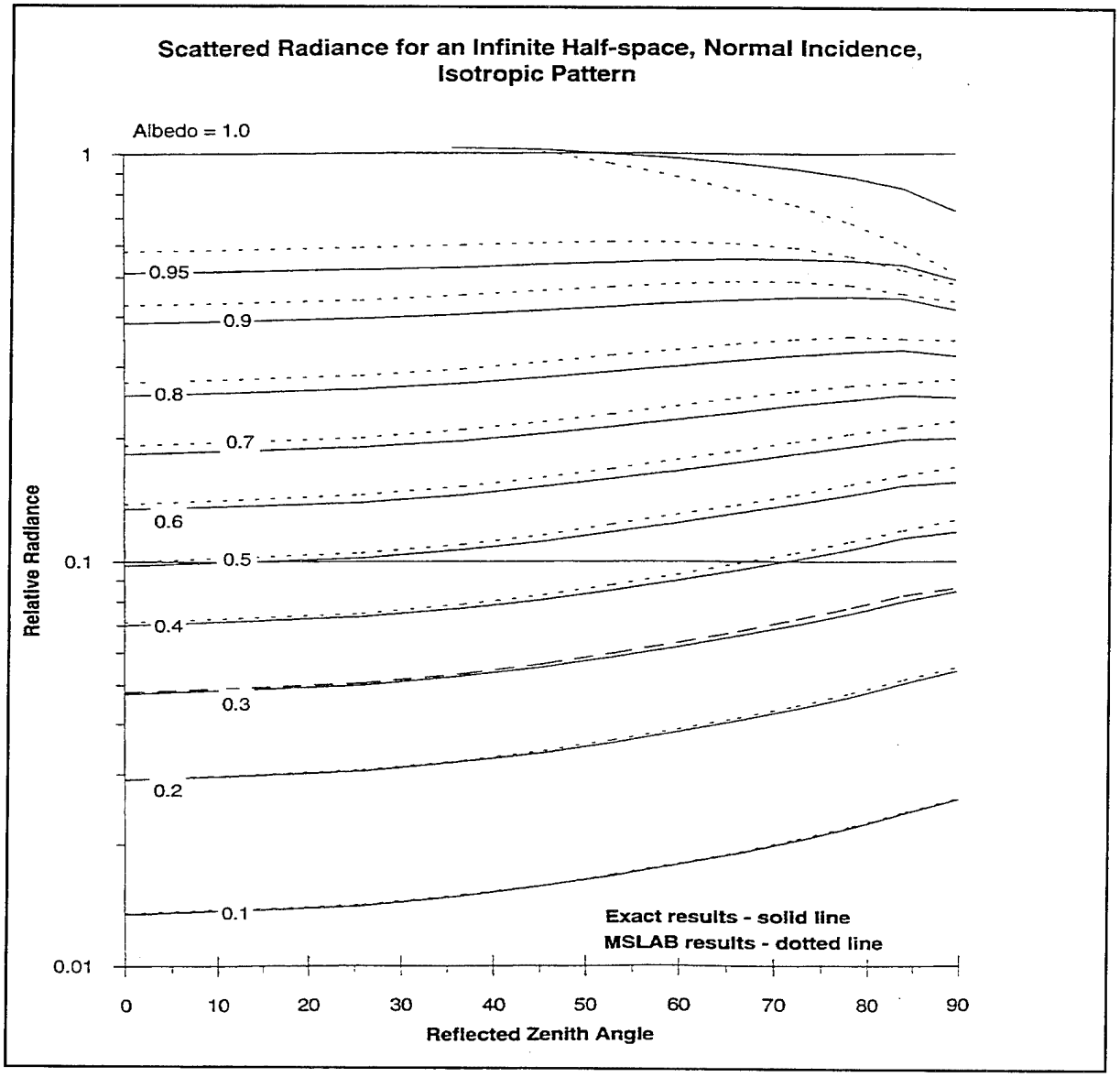

Figure 3. Comparison of MSLAB calculations to Chandraskhar's exact results.

Calculation of the Phase Function

Further work was done to compare MSLAB to an extensive set of calculations by Hansen (Hansen, 1971). Hansen combined Mie calculations with a doubling-method slab treatment to calculate phase functions, reflected radiance levels, and polarizations from clouds. Since his interest was in finding ways of using reflected sunlight to determine cloud microphysical properties, he chose for his calculations wavelengths in the shorter end of the IR and in window regions. His four wavelengths were at 1.2, 2.25, 3.1 and 3.4 μm. For his cloud droplet distributions he used the gamma distribution, which is obtained from the modified gamma distribution by setting γ to 1. He also parameterized the distribution using the quantities R_{eff} and σ^2_{eff}, which also appear as a and b in his paper. R_{eff} is the mean droplet radius, averaged over radius with the weighting function $\pi r^2 n(r)$. σ^2_{eff} is the variance. They can be converted to the modified gamma distribution parameters r_0 and a using the following relationship

$$r_0 = \sigma^2_{eff}\, r_{eff}; \quad \alpha = \frac{1}{\sigma^2_{eff}} - 2 \qquad (31)$$

To test the Mie scattering section of MSLAB, we reproduced Hansen's calculations of the single scattering albedo and forward directivity. Table 4 shows Hansen's results. The calculations are done at the four different wavelengths and at four different values of R_{eff}. For each, σ^2_{eff} = 1/9. Table 5 shows the results from MSLAB. Comparing the two, one sees that the disagreement in albedo and forward directivity between the two codes is less than about 1%. The agreement could be easily improved by increasing the angular resolution at which MSLAB calculates the phase function.

Further verification of the Mie code is shown in Figs. 4 - 7, where the phase functions from MSLAB are compared at two wavelengths to those of Hansen. Figure 4 shows Hansen's plots for four different R_{eff}'s. The plots are displaced from each other by one order of magnitude for clarity. The short horizontal bars found on the curves mark where each crosses unity. At 1.2 μm, the complex part of the index of refraction is small, so there is little absorption inside the droplet. The phase function shows a strong forward diffraction peak, along with peaks at around 140° and 180° scattering angle, corresponding to the rainbow and glory features. Since rainbows are due to geometric optics effects, they are expected to be more pronounced for larger drops.

The MSLAB calculations in Figure 5 show that MSLAB reproduces the drop in the phase function to a minimum and the rise up to the glory at 180°. The rainbow shows up clearly in the 12 and 24 μm curves as well. Overall the phase function magnitudes compare well, even at the 0° peak. One feature that is not well reproduced is the sharpness of the forward peak. This is due to the fact that the calculations were done at 21 scattering angles whose cosines are equally spaced by 0.1 from 1 to -1. With the first two angles at 0 and 25 degrees, MSLAB lacks the resolution to pick up the sharp peak at 0 degrees. A slight modification of MSLAB could produce greater resolution. It should be pointed out that when MSLAB performs its scattering calulations, it modifies the 0° part of the phase function to have a value closer to Hansen's values at around 10°. This is appropriate since extreme forward scattering is handled by modifying the extinction coefficient, as explained above.

At 3.1 μm, the complex index is comparatively large, and there is little structure in the phase function except for the forward peak. The MSLAB results in Figure 7 show the same general features as Hensen's results in Figure 6. The magnitudes compare well, and the increase in slope in the forward peak with increasing R_{eff} is represented. The resolution in MSLAB below 25° is still less than one would like.

Table 4. Hansen's Phase Function Results (Adapted from Hansen's Table 2.)

Wavelength (μm)		1.2	2.25	3.1	3.4
Index of Refraction	n_r	1.323	1.290	1.426	1.449
	n_i	9.74×10^{-6}	3.04×10^{-4}	.1828	.01888
	$R_{effective}$ (μm)				
ω_0	3	.999706	.996541	.5148	.8661
	6	.999379	.9890757	.4909	.7285
	12	.998818	.981374	.5115	.6289
	24	.988038	.969260	.5264	.5668
	$R_{effective}$ (μm)				
$< \cos \alpha >$	3	.7804	.8412	.8843	.7659
	6	.8311	.8016	.9308	.7910
	12	.8550	.8495	.9479	.8898
	24	.8677	.8720	.9523	.9336

Table 5. MSLAB's Phase Function Results

Wavelength (μm)		1.2	2.25	3.1	3.4
Index of Refraction	n_r	1.323	1.290	1.426	1.449
	n_i	9.74×10^{-6}	3.04×10^{-4}	.1828	.01888
	$R_{effective}$ (μm)				
ω_0	3	.999701	.996482	.5148	.8634
	6	.999359	.990535	.4908	.7259
	12	.996479	.976979	.5178	.6014
	24	.987868	.965257	.5284	.5615
	$R_{effective}$ (μm)				
$< \cos \alpha >$	3	.7902	.8511	.8959	.7694
	6	.8293	.8115	.9401	.8049
	12	.8737	.8561	.9537	.9105
	24	.9186	.8712	.9543	.9438

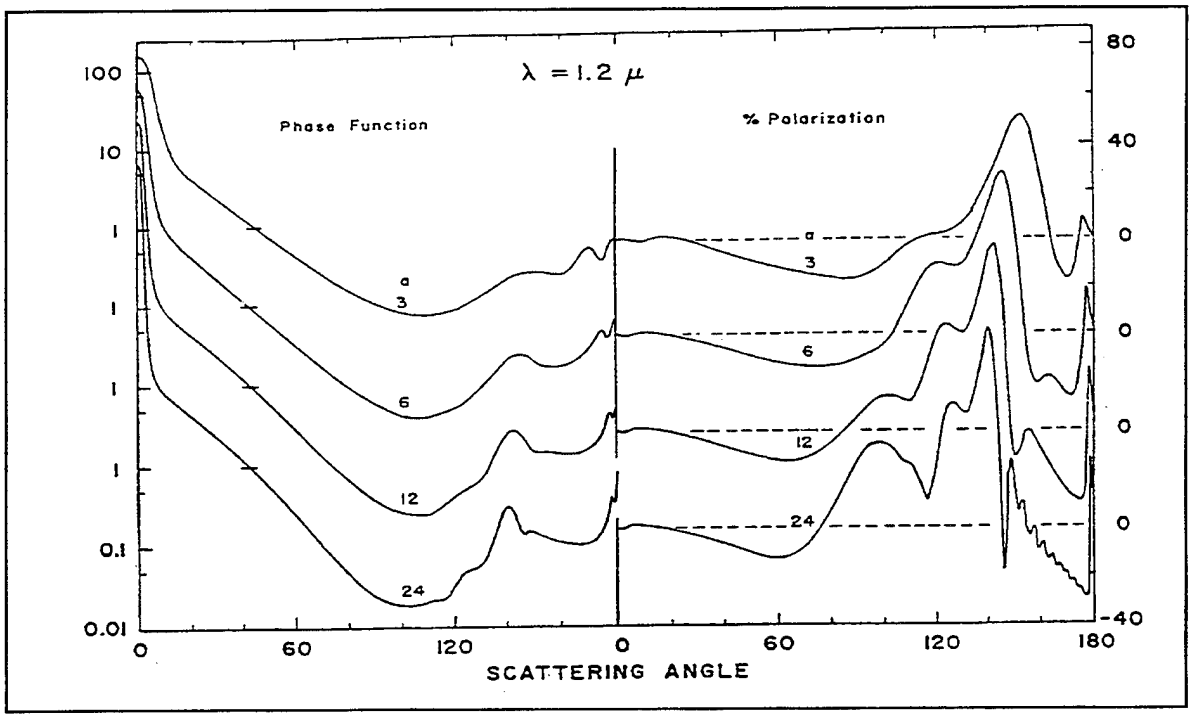

Figure 4. Hansen phase functions at 1.2 microns. Note that the horizontal bars are where each plot cross unity. (Hansen's Fig. 3)

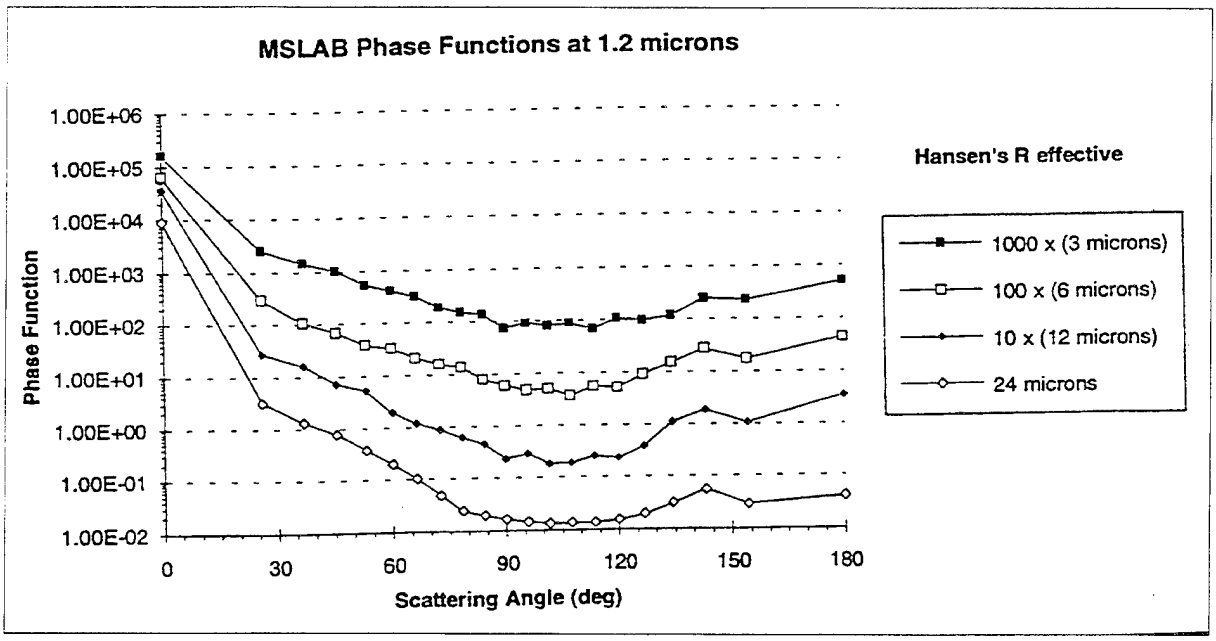

Figure 5. MSLAB phase functions at 1.2 microns

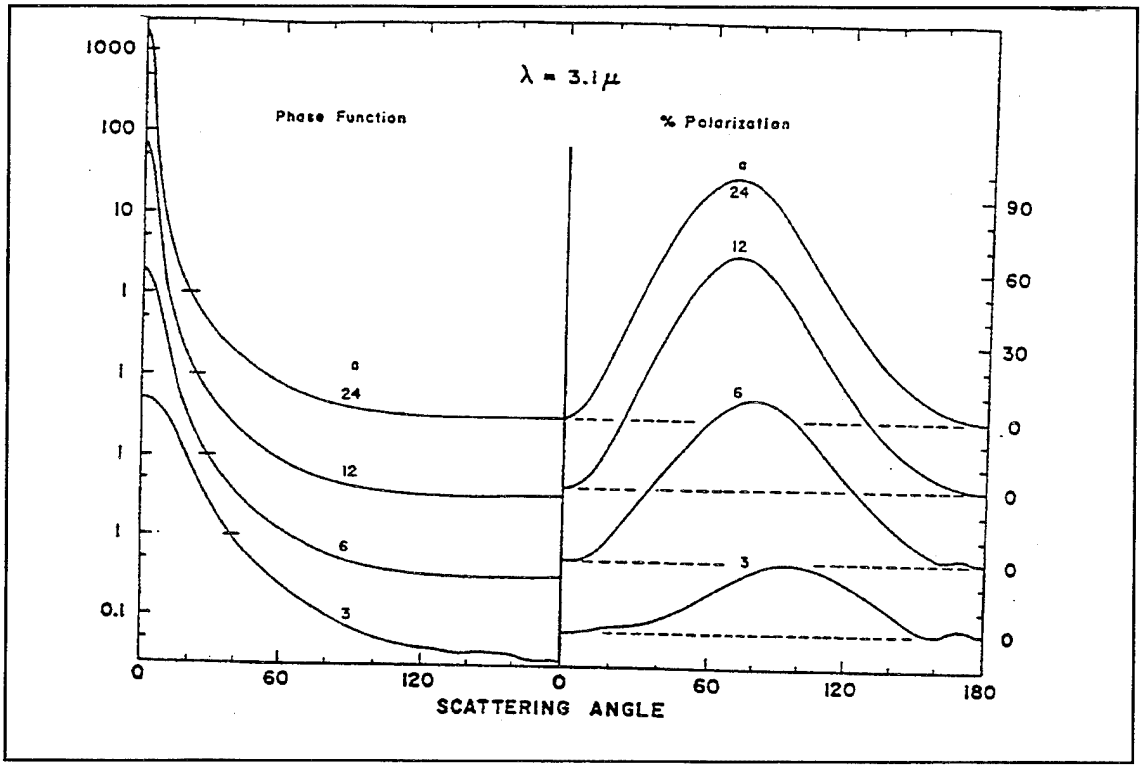

Figure 6. Hansen phase functions at 3.1 microns. Note that the horizontal bars are where each plot cross unity (Hansen's Fig. 6)

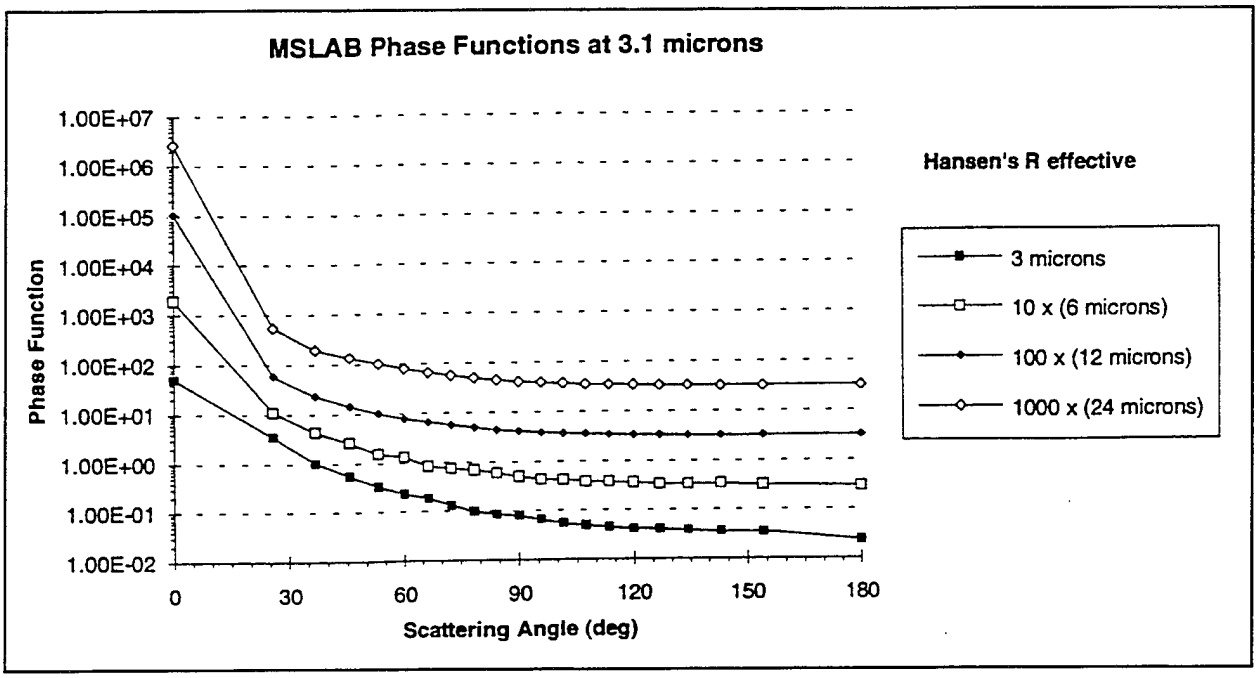

Figure 7. MSLAB phase functions at 3.1 microns

Optical Depth Variations

Figures 8 through 13 compare the BRDF values calculated for different optical depths by Hansen and MSLAB. The Hansen calculations were done using $R_{eff} = 6$ μm and $\sigma^2_{eff} = 1/9$, while MSLAB used a distribution that PRA has employed in the past to model altostratus clouds: $R_{eff} = 6.49$ μm and $\sigma^2_{eff} = .08$. (Mertz, 1991a). All calculations were done at 0 solar zenith angle. Figure 8 shows Hansen's reflected intensity results at 1.2 μm. The normalization of his results is such that it is equal π times a BRDF. Figure 9 shows the MSLAB results suitably normalized for comparison. The rainbow peak in the phase function at about 140° scattering angle shows up as a peak in the BRDF at around 40° observer zenith angle for small optical depths in both figures. This feature is washed out as the optical depth increases. Figure 9 also shows CLDSIM's alto4.db BRDF at its nearest wavelength to 1.2 μm. The curve shows that the CLDSIM BRDF corresponds to a large optical depth cloud. (The alto4.db file gives the optical depth as about 44 for this wavelength.)

Figure 10 shows Hansen's results at 3.1 μm. The smoothness of the phase function at this wavelength is reflected in the smoothness of the BRDF. The peaking of the BRDF at 90° observer zenith angle - especially for small optical depth - is the result of reflection off of the water droplets. These features show up in MSLAB's results in Figure 11. The curves from

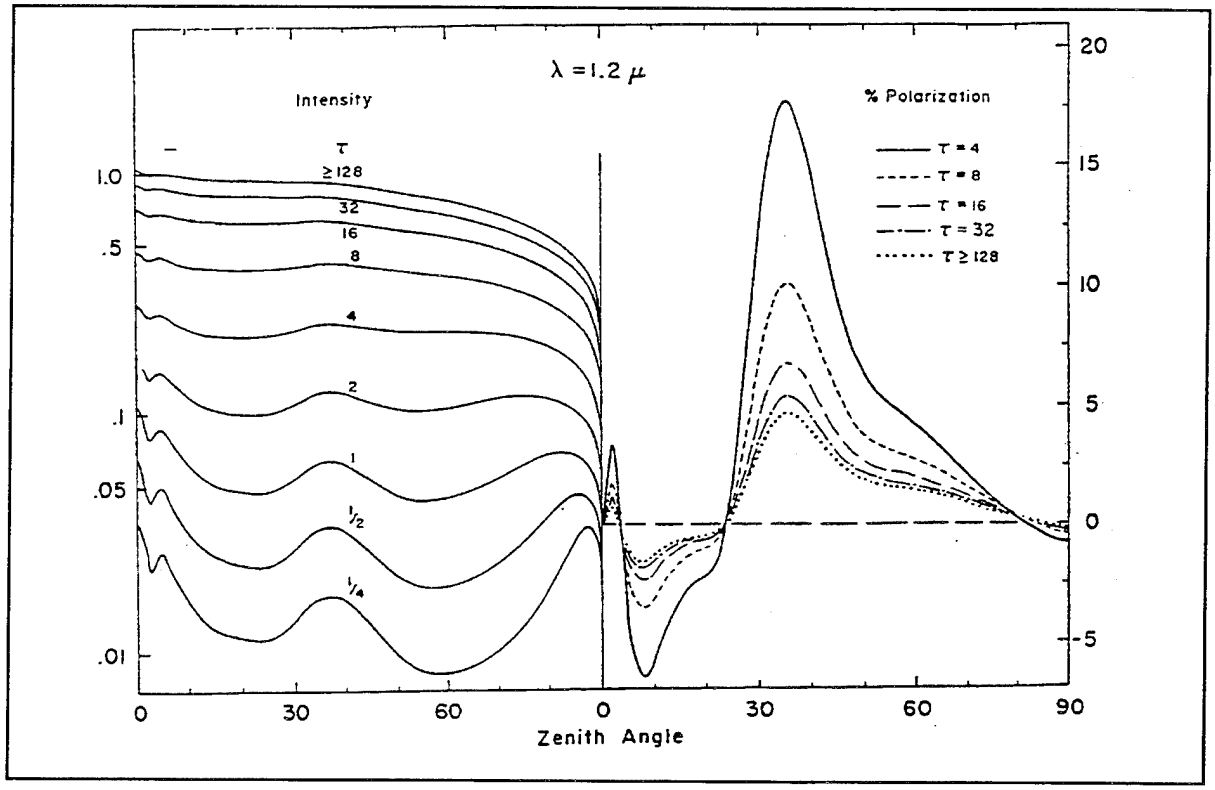

Figure 8. Hansen optical depth variations at 1.2 microns (Hansen's Fig. 7)

CLDSIM's alto4.db at two bounding wavelengths are also shown and compare well to MSLAB. Close examination of the ordinates of Figs. 10 and 11 show a factor of ten difference between Hansen on the one hand and CLDSIM and MSLAB on the other. Due to the close agreement of the later two codes, there is likely to be a typographical error in Hansen's plot. Figures 12 and 13 show Hansen's and MSLAB's results at the nearby wavelength of 3.4 μm. The agreement is good except at small zenith angles where MSLAB needs more resolution.

Particle Size Variations

Hansen investigated the effect of changing the particle size distribution on BRDFs. Figures 14 and 16 show his results for distributions which have the same σ^2_{eff} value of 1/9, but differ in their R_{eff} parameter, which appears as "a" on the plots. The optical depth is 32 for each curve. Since this value corresponds to a thick cloud, variations seen in these plots can be viewed as conservative. At 1.2 μm, one sees the rainbow peak become visible around 40^0 observer zenith angle for the large droplet distributions. For these distributions, the scattering is sufficiently into the geometric optics regime to allow the rainbow to appear even for thick clouds. Figure 15 shows the MSLAB results, which agree well for sizes below 24 μm.

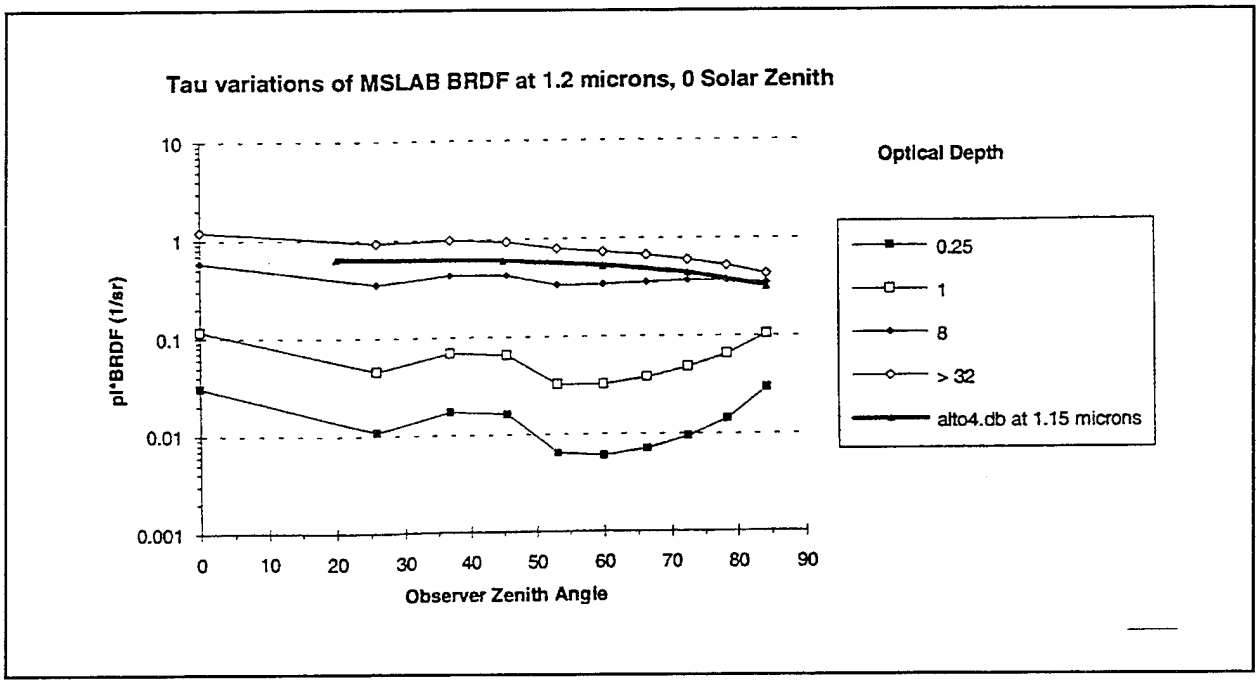

Figure 9. MSLAB optical depth variations at 1.2 microns

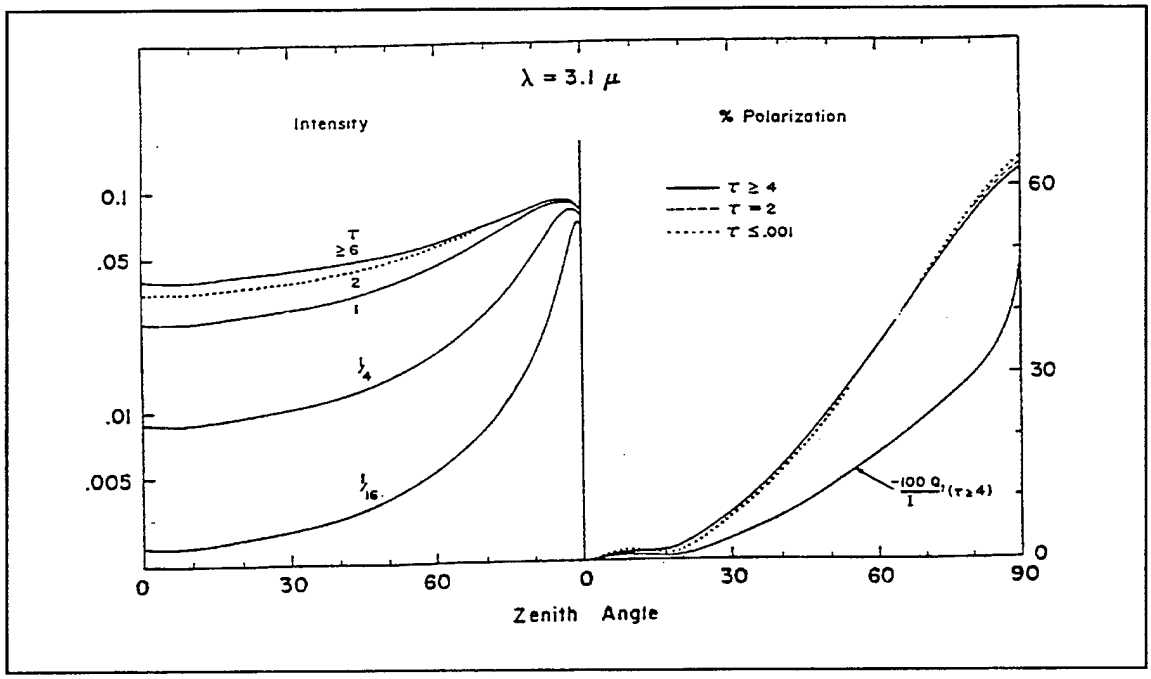

Figure 10. Hansen optical depth variations at 3.1 microns (Hansen's Fig. 10)

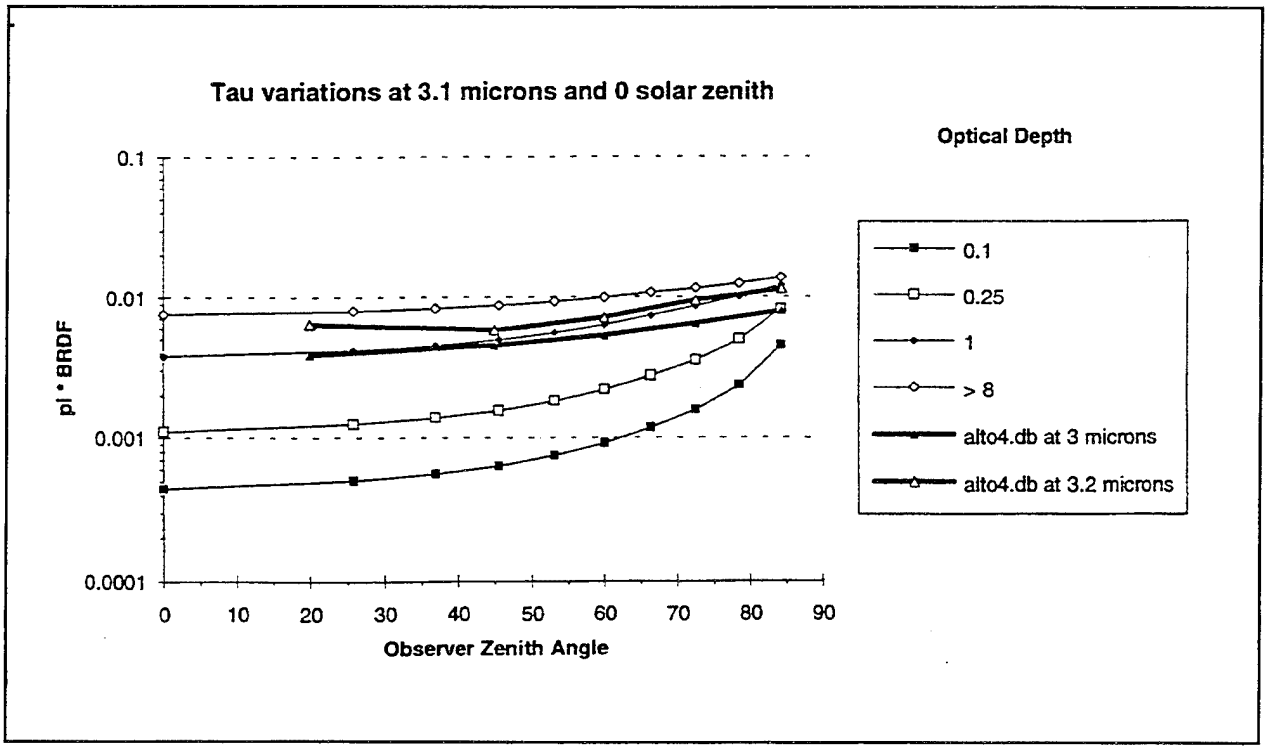

Figure 11. MSLAB optical depth variations at 3.1 microns, with CLDSIM's alto4.

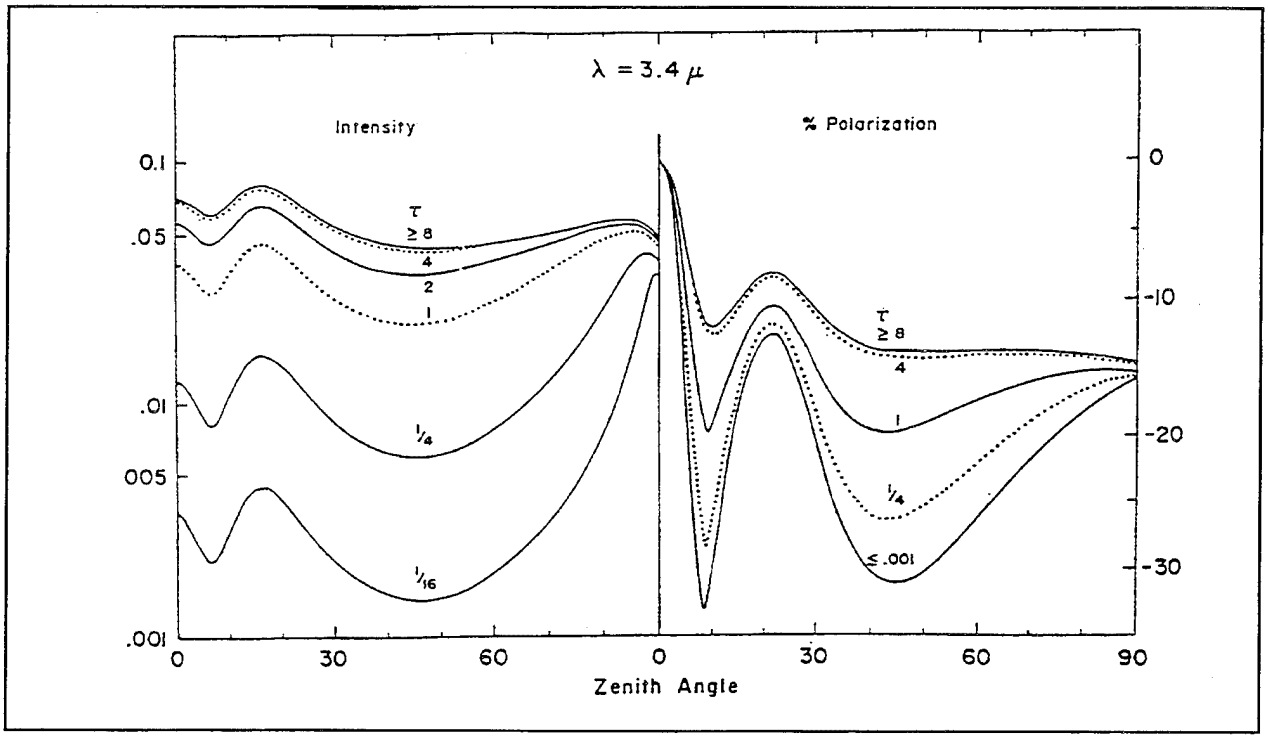

Figure 12. Hansen optical depth variations at 3.4 microns (Hansen's Fig. 11)

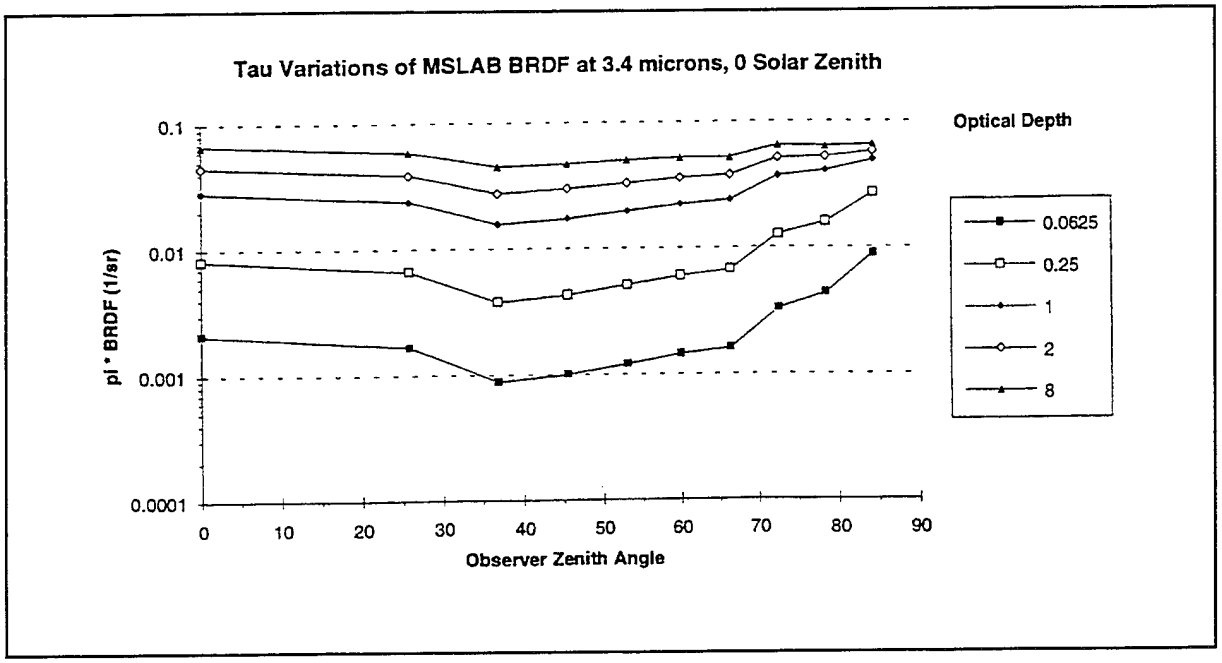

Figure 13. MSLAB optical depth variations at 3.4 microns

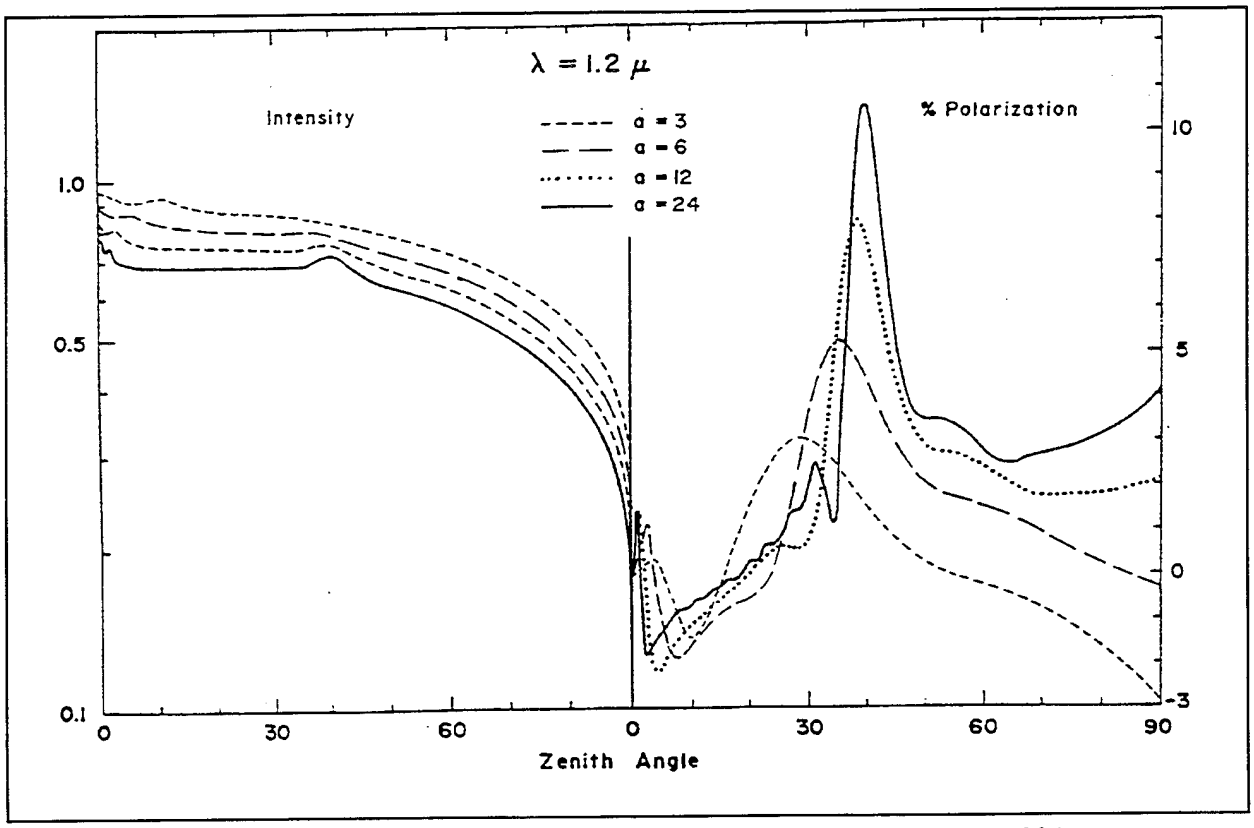

Figure 14. Hansen particle size variations at 1.2 microns (Hansen's Figure 20.)

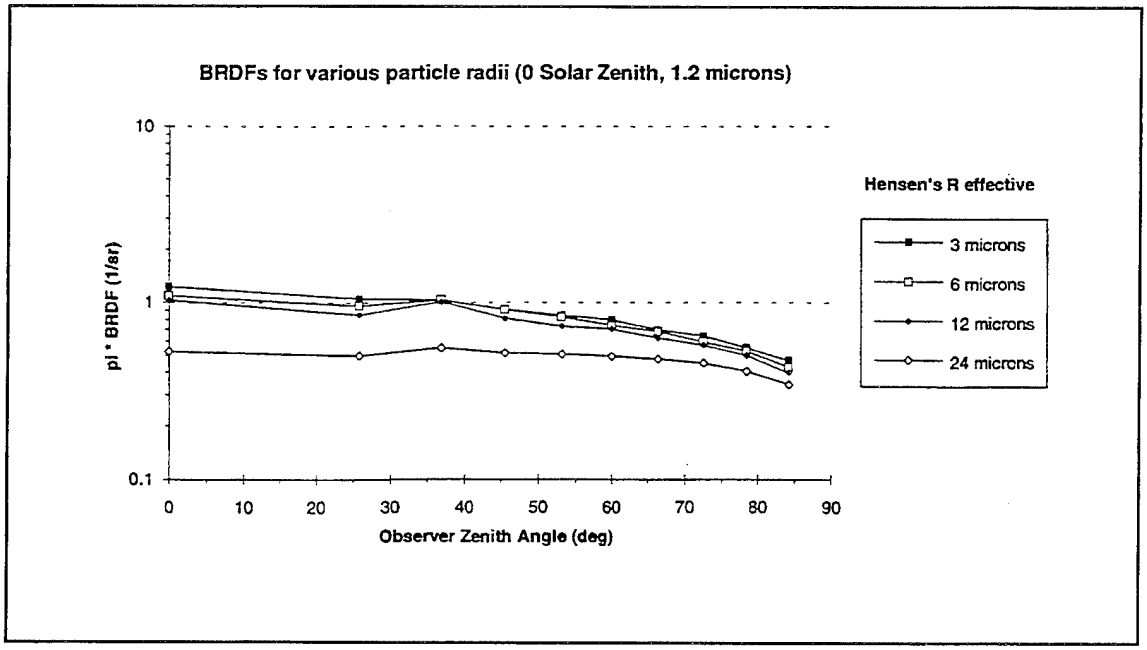

Figure 15. MSLAB particle size variations at 1.2 microns

Figure 16 shows Hansen's results at 3.4 μm. The decrease in BRDF with inceasing R_{eff} comes from the greater absorption of light traveling through larger droplets. The SLAB results in Figure 17 reproduce the flat distribution of R_{eff} = 3 μm, and the rising tails of the other distributions. The plot lacks enough angular resolution below 25^0 to pick up the structure seen in Hansen's work.

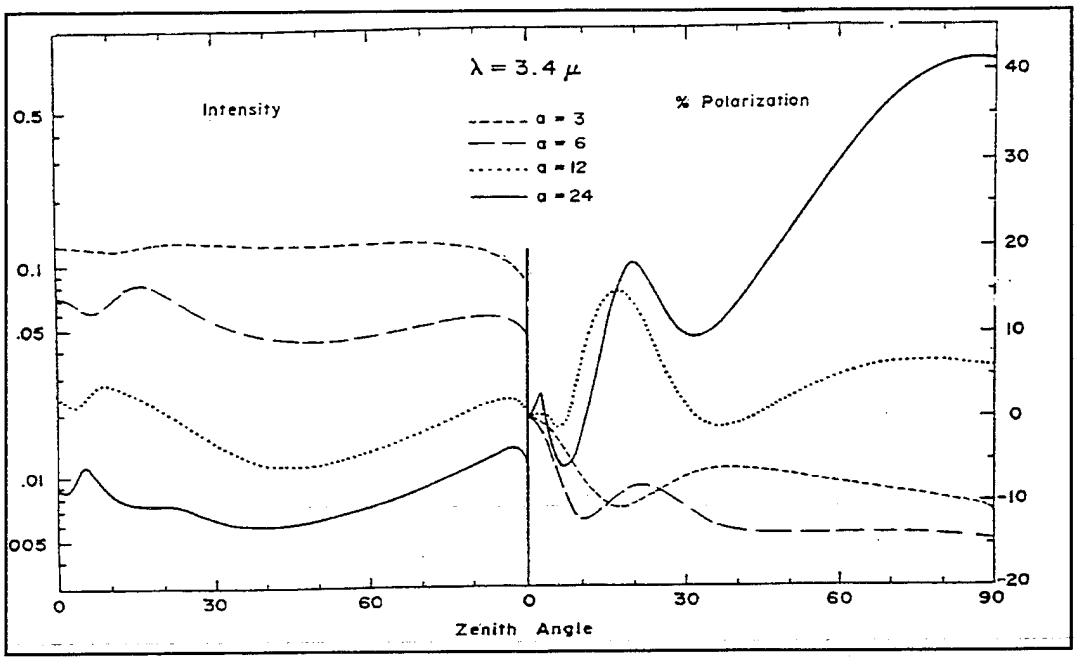

Figure 16. Hansen particle size variations at 3.4 microns. (Hansen's Fig. 21.)

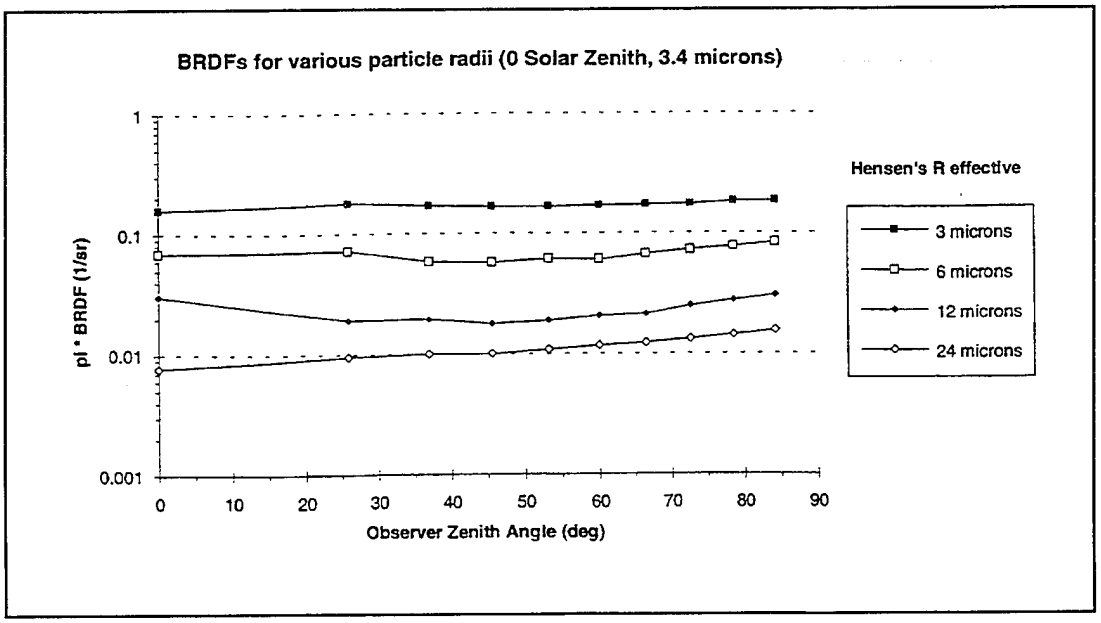

Figure 17. MSLAB particle size variations at 3.4 microns.

Gaseous Absorption

Hansen's work emphasized window regions without significant gaseous absorption. It is important to validate MSLAB in absorbing regions. To date, the only validation that has been done has been to follow PRA's lead and compare MSLAB to the work of Futterman that is cited in (Mertz, 1991a). In that paper, a calculation of the BRDF of a Fair Weather Cumulus cloud at 2.7 μm is shown with and without gaseous absorption included. It is reproduced here in Figure 18, while Figure 19 shows the MSLAB results. Both show that the major effect of adding gaseous absorption at this wavelength is to reduce the value of the BRDF by a factor of about 4 for Futterman's results and about 2.5 for MSLAB, without significantly affecting its angular dependence. Besides this, there is some difference between the overall level of the MSLAB BRDF and that of Futterman.

Two conditions may help to explain this difference. First, there was not enough information provided in PRA's paper to reproduce the particle distribution of the Futterman cloud. MSLAB used instead a standard particle distribution that PRA has employed in the past to represent cumulonimbus clouds (72 drops/cm^3, R_{eff} = 14, σ^2_{eff} = .113), even though it did not compare closely with the information provided about Futterman's distribution. Using this distribution, MSLAB predicted a single scattering albedo (without gaseous absorption) of 0.53, which is smaller than Futterman's value of 0.76. This suggests that the MSLAB distribution will produce lower BRDFs than Futterman predicts even before gaseous absorption is considered.

Another factor that may effect the result is that CLDSIM's BRDFs are computed by expressing gaseous absorption as a series of exponentials, each containing a different gaseous absorption coefficient. A BRDF is computed for each term in the series, and they are averaged to produce the final result. (See equations 4 and 5) MSLAB only uses a one-exponential approximation, although going to multiple exponentials would not be difficult to do. In sum, Figs. 18 and 19 show that MSLAB predicts reasonable BRDFs in absorption bands, although it is not fully validated there.

Conclusion

The validation of MSLAB has shown that its Mie code is able to reproduce phase functions and albedos to a degree of accurary presently limited only by the its angular resolution. The validation has also shown that MSLAB can reproduce the dependence of BRDFs on wavelengths and particle sizes. Although its treatment of gaseous absorption is not fully validated, MSLAB does produce reasonable results in absorption regions.

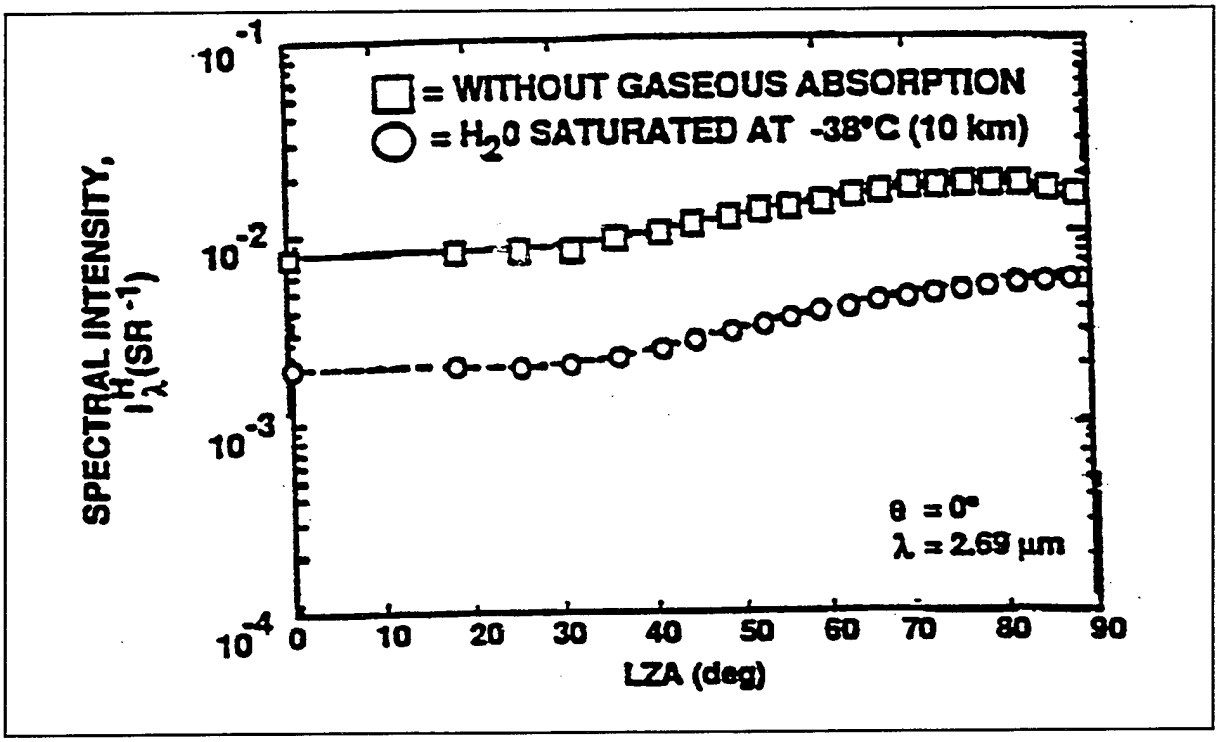

Figure 18. Futterman's BRDFs with and without gaseous absorption
(From Mertz, 1991a, Fig. 4.28)

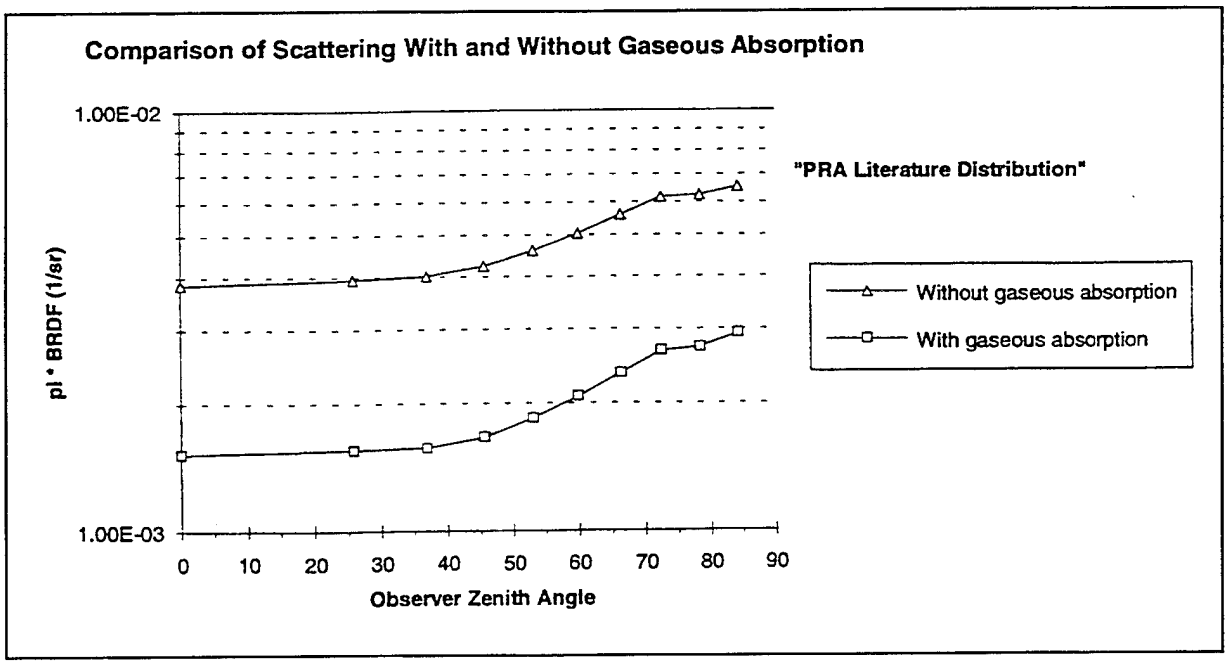

Figure 19. MSLAB BRDFs with and without gaseous absorption

3.3 Critique of PRA BRDF Methods

Small Optical Depth Treatment

PRA's MSRAT BRDFs are calculated for clouds with large optical depths. Lines-of-sight through clouds to the ground may have small optical depths, either because they intersect a thin cloud "puff" or the edge of a thick cloud. In addition, if lower elevation geometries become more important, the shadowing of parts of one cloud by another can occur, in which case shorter path lengths and small optical depths come into play.

Because each of CLDSIM's BRDFs is precomputed at one optical depth, CLDSIM handles small optical depths using the simple formula

$$\rho_\tau = (1 - e^{-\tau})\,\rho \qquad (32)$$

Figures 20 and 21 compare this method with calculations done using MSLAB. The MSLAB BRDFs were made using gamma distribution parameters for an altostratus cloud and represent the situation shown in Hansen's Figs. 8 and 10 above. Note that at 1.2 μm, the MSLAB results show much more structure around the rainbow position for small optical depth than for large. The effect of CLDSIM's approximation is simply to translate the large optical depth BRDF to smaller values in a log plot. Thus, this method does not change the BRDF's shape to show more structure. Note also that the overall separation between the curves with optical depth 0.25, 1, and 8 is much greater than the separation predicted by CLDSIM's approximation. As a sensor scans over an area with clouds, it will see jumps in radiance as the line-of-sight enters or leaves a cloud. These jumps will be smoothed out some by the decreased opacity of the cloud near the edges. By overpredicting the radiance for small optical depths, CLDSIM accentuates the cloud/non-cloud transition, and increases the predicted clutter for the sensor.

Figure 21 shows the results at 3.4 μm. At this wavelength, absorption inside water droplets produces a smoother and dimmer BRDF. The smoothness of the BRDF makes CLDSIM's approximation more appropriate here than at 1.2 μm, although CLDSIM still does not predict the increase in the fraction of radiance at 90^0 observer zenith angle seen at smaller optical depths. Because of the smooth BRDF and the drop off in solar inradiance at this wavelength, conditions at 3.4 μm are not as stressing to a sensor as conditions at 1.2 μm.

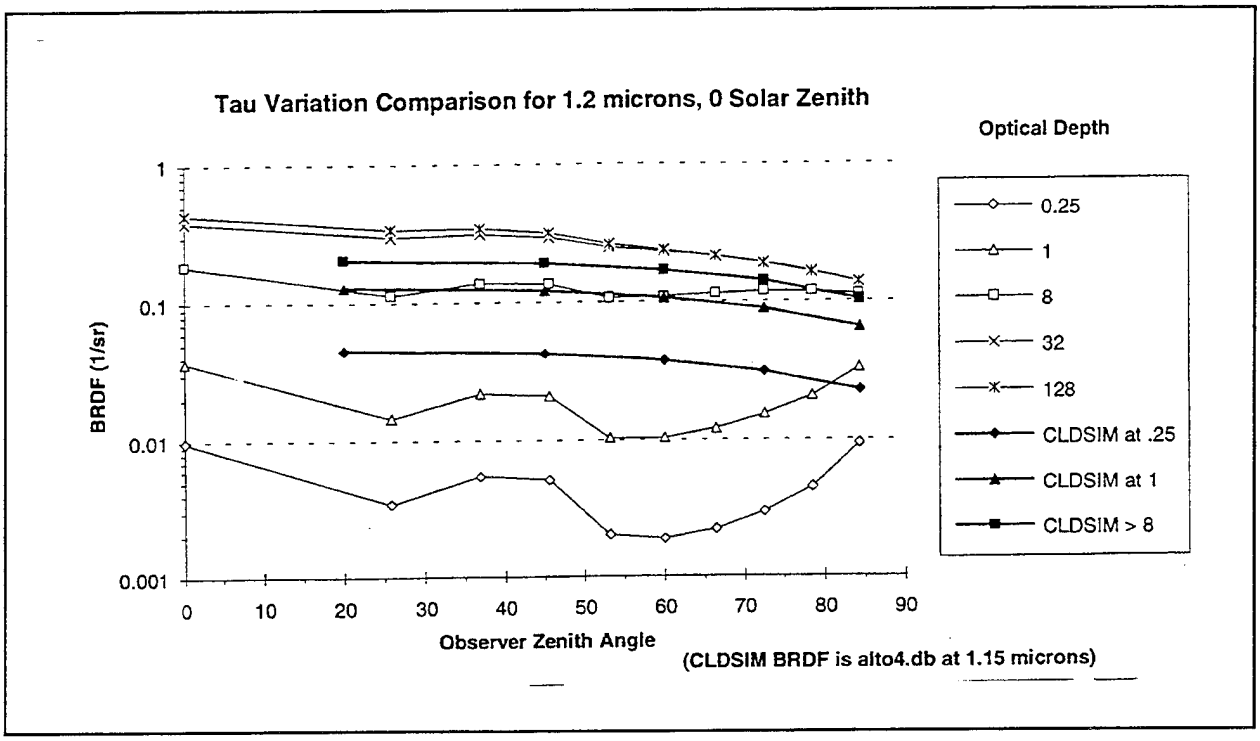

Figure 20. Comparison of optical depth compensation methods at 1.2 microns

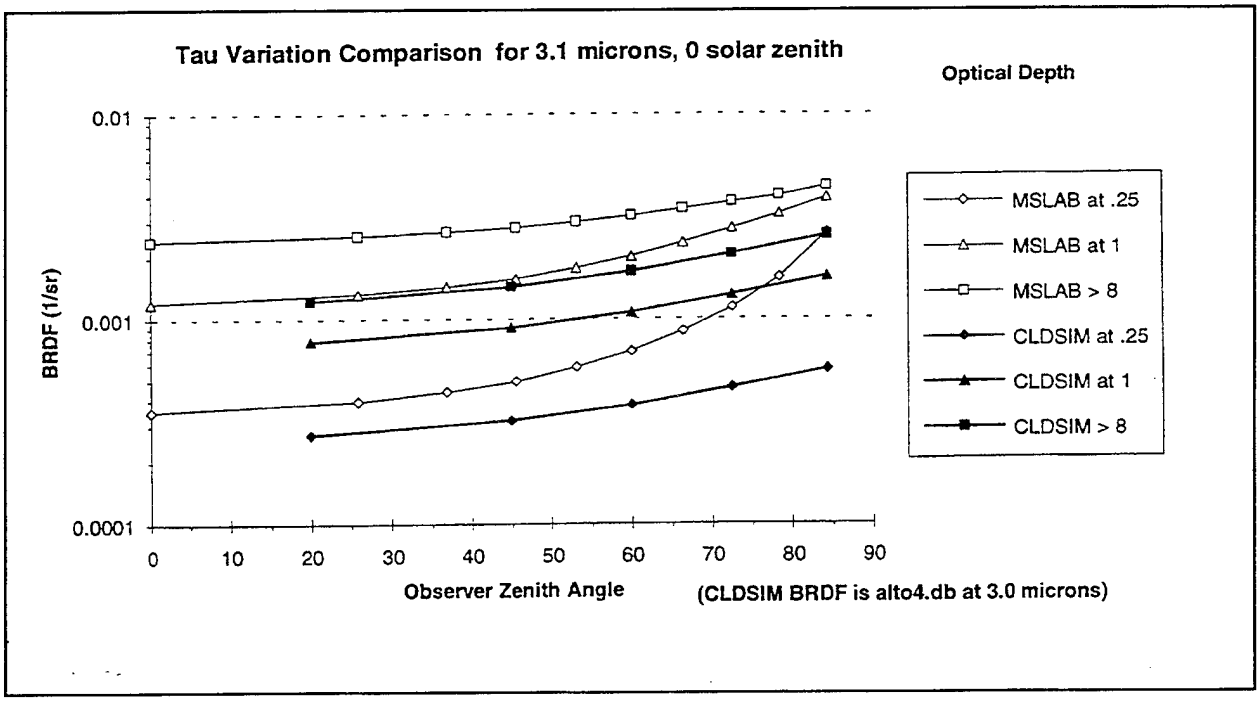

Figure 21. Comparison of optical depth compensation methods at 3.1 microns

4. CORRELATED LINE TRANSMISSION EFFECTS

Our review of CLDSIM modeling noted the careful treatment of atmospheric absorption. The spectral bands selected for a number of important satellite surveillance systems are centered in the strong atmospheric absorption bands of CO_2 and H_2O. There are a variety of reasons for this, not the least of which is the desire to eliminate clutter from the earth surface. In any case, determination of the transmission in such spectral regions poses a significant challenge to the modeller.

CLDSIM utilizes the band model program APART to calculate the transmission through the atmosphere along the "dogleg" paths from the sun to cloud surface and from cloud surface to observer. Note that the transmission cannot be calculated for each segment of the dogleg path and then multiplied since the (inherent) spectral average does not commute with the path integral. CLDSIM actually uses a set of such dogleg paths spanning the range of possible cloud surface facet locations. CLDSIM interpolates this database for each specific cloud scattering facet location.

Although CLDSIM treats solar scattering as a surface phenomenon, it is in fact a volume one. Recognizing this, the CLDSIM developers included gaseous (vapor) absorption in the calculation of the cloud BRDFs. At Visidyne's review meeting with them they indicated that without the vapor absorption the predicted radiances were much too high in calculations for absorption band regions.

In CLDSIM, the cloud vapor absorption is treated independently of the atmospheric absorption, thereby in effect multiplying the transmissions. Multiplication of transmissions ignores the correlation of absorption lines in the segments involved and leads to an overestimate of the absorption loss. This can be seen in Figure 22 which shows one of the CLDSIM validation plots, redrawn from Figure 11 of Blasband and Jafolla (1990). The cloud is a cirrus cloud at 11 km altitude. The zenith angle of the sun is 59° and that of the observer is 80°. The authors note that the band integrated radiances compare reasonably well, 6.4 x 10^{-7} W/cm^2/sr for the A.D. Little data versus 9.2 x 10^{-7} for the CLDSIM calculation. However, CLDSIM overestimates the depth of the absorption in the band centers, a fact that is consistent with the neglect of the correlation of absorption in the atmosphere and cloud vapor.

To estimate the magnitude of the error in neglecting the correlation of atmospheric path and cloud vapor absorption, Visidyne used the ATHENA LTE band model code (DeVore,1987) to model two simple cases involving clouds at 5 and 11 km altitude. We

assumed a vertical path down through the atmosphere, a specific distance through the cloud, and then back vertically up through the atmosphere. We compared calculations of the transmissions for paths in the cloud only, down and up through the atmosphere only, and through the atmosphere and the cloud. The results are presented below.

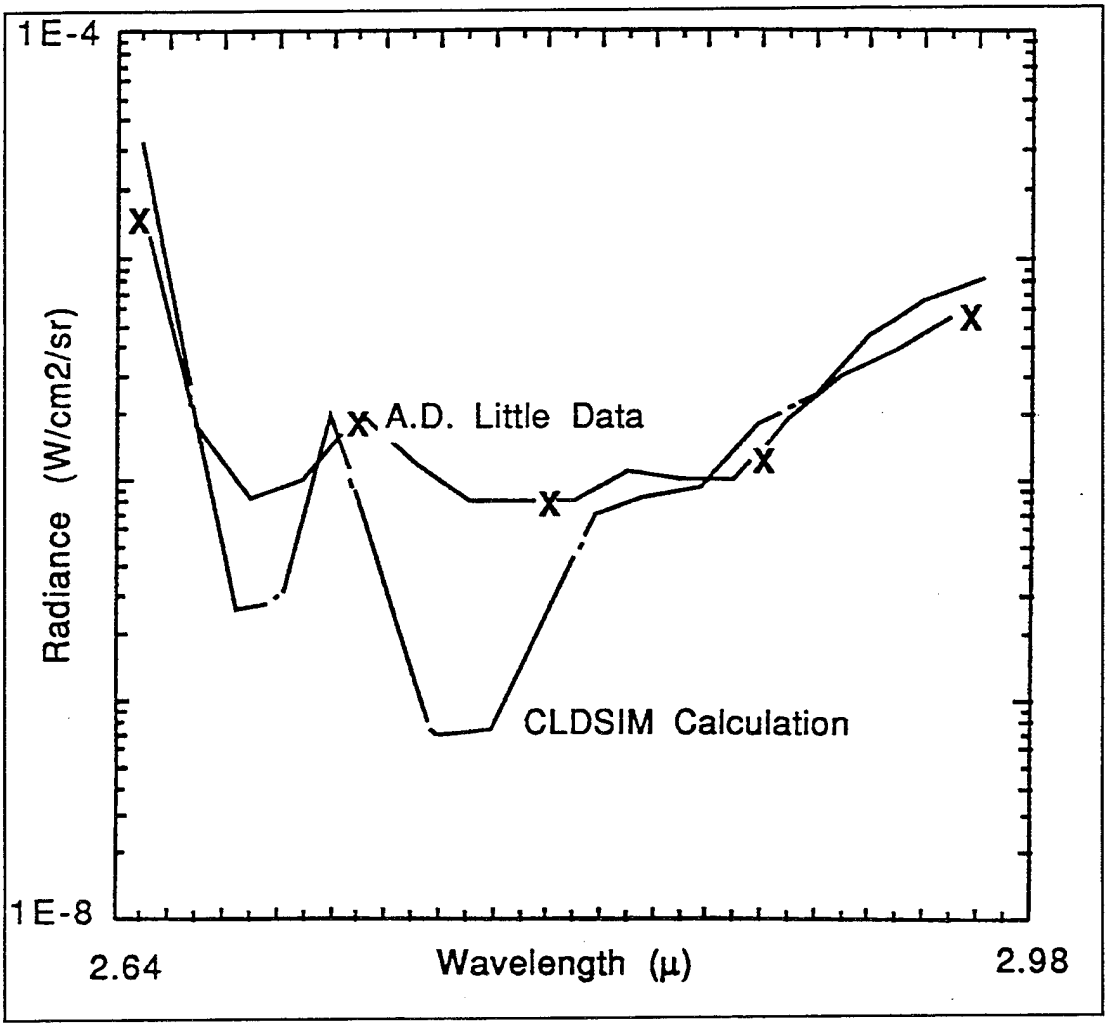

Figure 22. Comparison of CLDSIM calculation with A.D. Little aircraft data, redrawn fromBlasband and Jafolla (1990).

5 Km Cloud Case

For the first case we considered a typical cloud at 5 km altitude. Figure 23 shows altitude profiles of the primary atmospheric absorbers in the SWIR and the atmospheric temperature. The path length in the cloud is selected so that the absorption in the band centers is

approximately a tenth, as shown in Figure 24. This figure also shows the absorption in the atmosphere and in the combined atmosphere-cloud system. Note that the transmission differences in the band centers between the atmosphere only and the combined atmosphere-cloud system are less than the cloud only transmission. Because of this, the process of treating the cloud and atmospheric transmission as uncorrelated by simply multiplying them together underestimates the total transmission. This is seen in Figure 25, which compares the correlated transmission calculated for the combined system with the uncorrelated product of the transmissions for the separate atmosphere and clouds. CLDSIM uses the uncorrelated method of combining transmissions. The relative error of this method can be estimated by taking the ratio of the two types of transmission calculations as is done in Figure 24. This figure shows that neglecting line correlation can lead to overestimates of transmission loss by up to a factor of 30 (at 2.68 μm, for instance). Of course, the magnitude of the error depends upon the specifics of the case.

11 Km Cloud Case

We performed a similar set of calculations for a 11 km altitude cloud, such as was observed in the A.D. Little data. Figure 27 shows the results of the transmission calculations, while Figure 28 shows the relative error involved in neglecting line correlation. Note that in this case the transmissions are much larger in the band centers as should be expected at the higher altitude here. Because of this, the error is much smaller, e.g., a factor of 3.

Conclusions

The calculations described above indicate that neglect of line correlation can lead to overestimates of transmission loss by up to a factor of 30 in middle level clouds (5 km) and a factor of 3 for high level clouds. The band-averaged differences ranged from over a factor of 2 to slightly less than 50 %. These figures should not be taken as definitive, since (a) they refer to two specific cases and (b) the model was as simple as we could make it. However, the calculations are consistent with the idea that discrepancies between the A.D. Little data and the CLDSIM calculations shown in Figure 22 can be attributed to CLDSIM's neglect of the line correlation between the atmospheric path and cloud vapor transmissions.

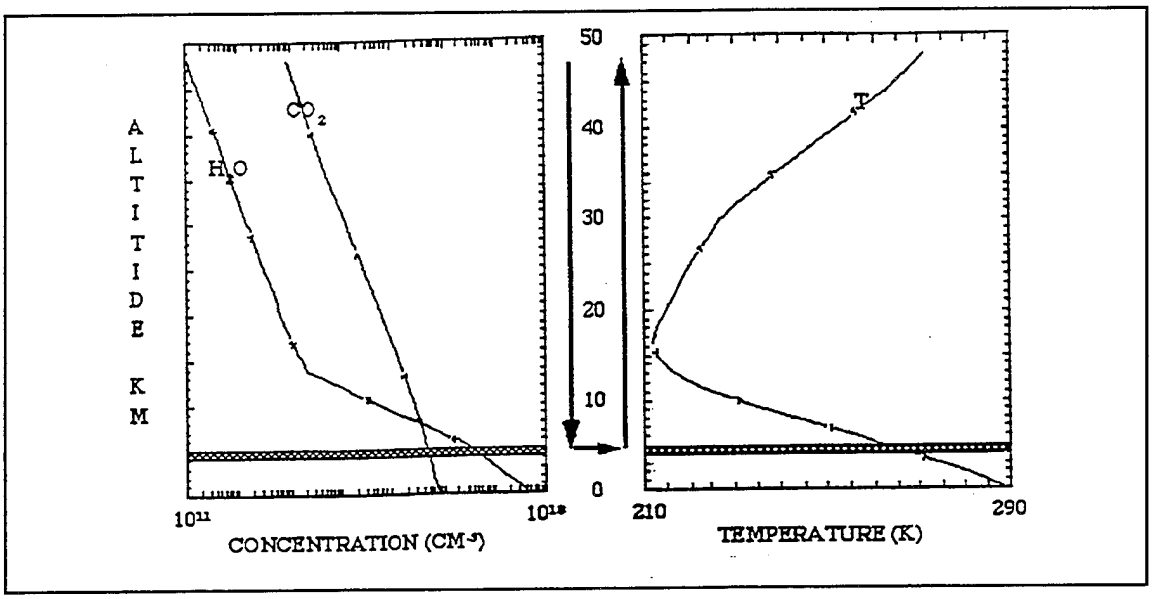

Figure 23. Atmospheric Profiles for the 5 km cloud case

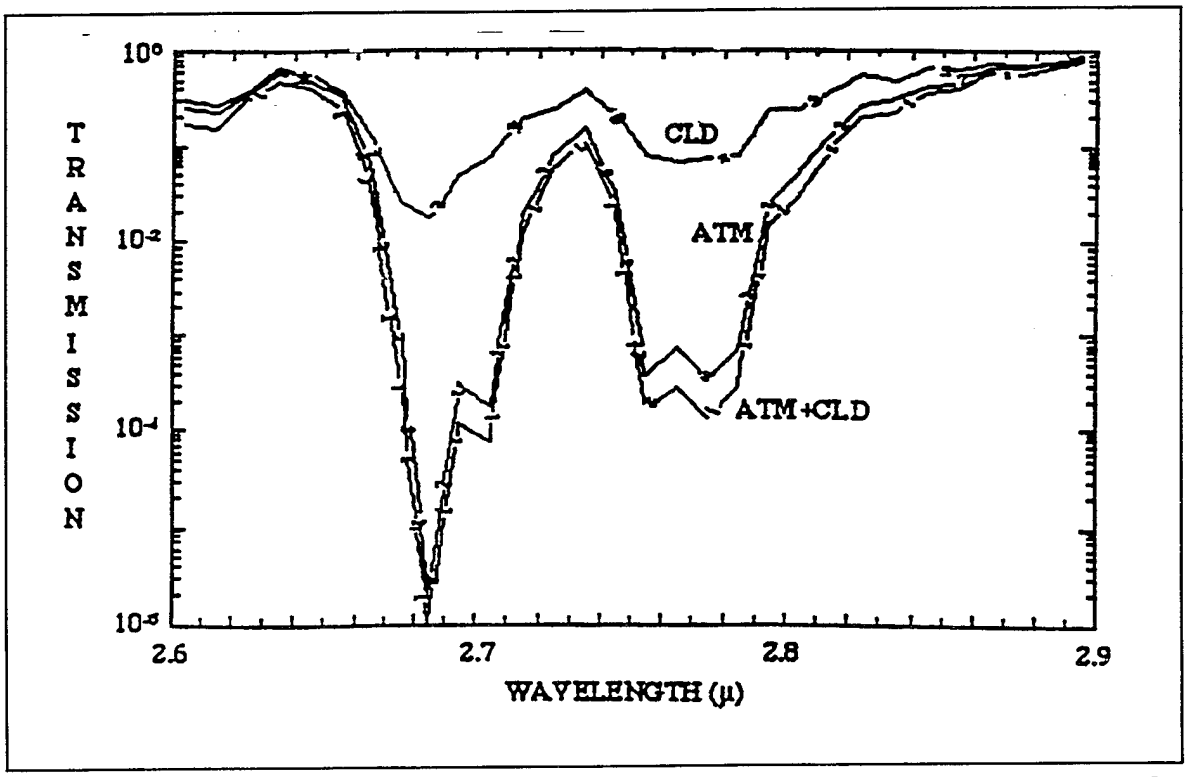

Figure 24. Calculations of the transmission in the cloud (CLD), in the atmosphere only (ATM), and in the atmosphere plus cloud (ATM+CLD)

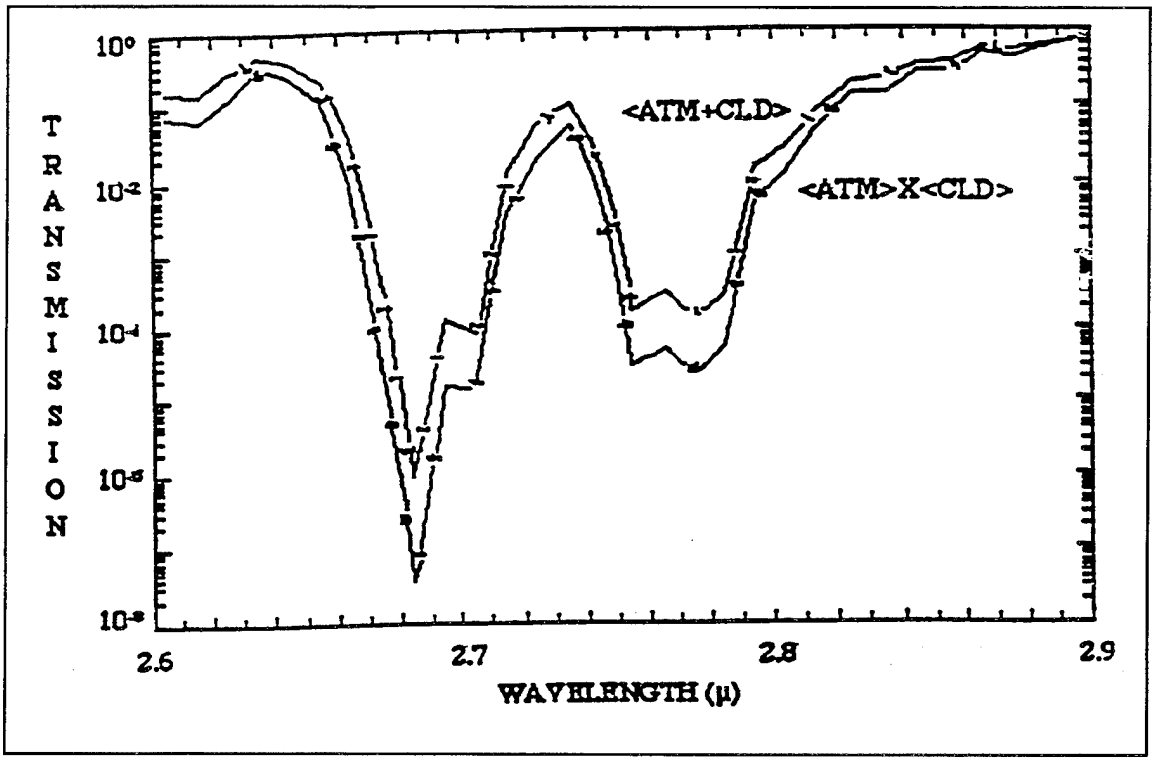

Figure 25. Comparison of the correlated transmission calculation (< ATM+CLD>) with an uncorrelated product calculation (<ATM> x <CLD>).

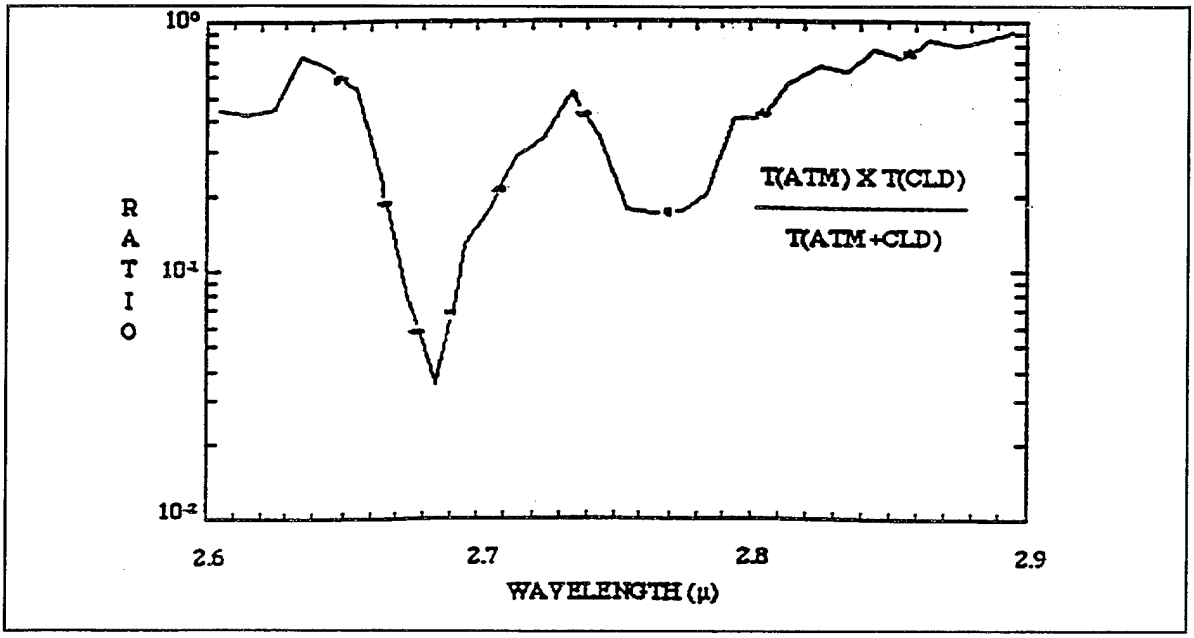

Figure 26. Relative error in using the product of the atmospheric and cloud transmissions rather than the combined atmosphere-cloud transmission

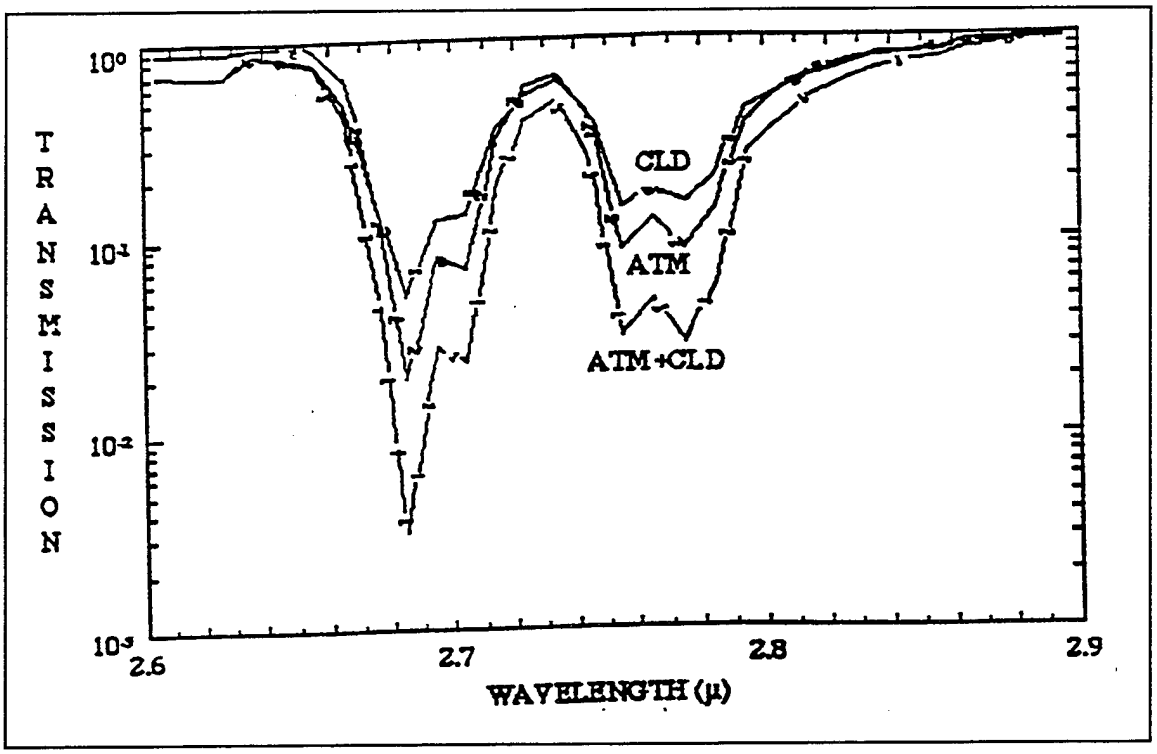

Figure 27. Calculations of the transmission in the cloud (CLD), in the atmosphere only (ATM), and in the atmosphere plus cloud (ATM+CLD)

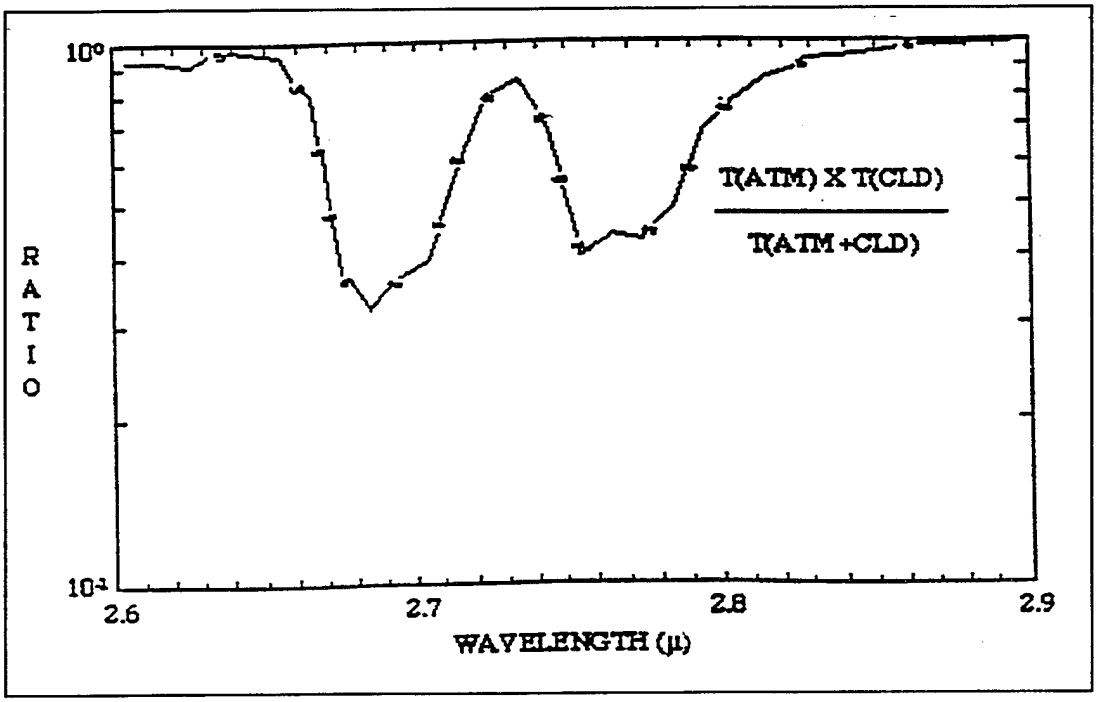

Figure 28. Relative error in using the product of the atmospheric and cloud transmissions rather than the combined atmosphere-cloud transmission.

5. CONCLUSIONS AND RECOMMENDATIONS

Throughout the course of the CLDSIM review, the high quality of PRA's work has been evident. The extent to which PRA has taken pains to validate CLDSIM is especially commendable. However, a few general comments can be made about CLDSIM. They are followed by more specific recommendations.

CLDSIM has been used in the past to simulate radiances seen by high altitude strategic surveillance sensors observing large regions at moderate spatial resolution. More recently, it is being used to model returns for high-resolution theater scenarios. To accommodate this new mission, some of the assumptions made in the CLDSIM model should be modified. For instance, CLDSIM's shadowing treatments should be updated to improve cloud-to-cloud interactions. In addition, scattering off of smaller cloud features should be enhanced by new methods of treating small optical depth BRDFs.

CLDSIM has also evolved from a stand-alone tool used primarily by PRA personnel to a code readily available to the defense community through the SSGM. CLDSIM should be changed in at least two ways to better reflect this evolution. First, it presently has an architecture that sequentially processes whole databases, calculating surface normals on the first sweep through the database, scattering angles on the second, and radiances on the third. CLDSIM saves the results from each sweep. This architecture is an advantage in a stand-alone code where these intermediate results can be reused in slightly altered runs. For instance, a scattering angle file can be shared between two runs where only the assumed model atmosphere has changed. The saved intermediate results have little utility in the SSGM and in fact slow down its operation. A better architecture would be one that performs complete calculations on each pixel before moving to the next pixel, and one that processes only those pixels in the FOV.

The move from a stand-alone code to the SSGM has placed CLDSIM in the hands of less sophisticated users. Increased error checking should be added to CLDSIM to make sure that the complex mix of clouds, atmospheres and locations that go into a CLDSIM run are physically consistent. In addition, more information should be given about the meteorology represented in CLDSIM's clouds to help the user run the code in an intelligent manner.

Cloud Databases

1) The techniques used to spatially interpolate databases to finer resolution should be validated.

2) Methods to generate synthetic cloud altitude maps with realistic structure should be developed to supplement the cloud databases constructed from data.

3) Data should be collected on the range of returns seen by an operational sensor, for use in developing a metric whereby the structure in CLDSIM scenes could be classified as stressing or benign.

4) Sources of stereoscopic measurements of cloud altitudes and other techniques should be investigated to supplement or validate CLDSIM's predictions of clutter from the sides of clouds with large vertical development. The proposed RAMOS experiment could supply such measurements.

5) As PRA suggested, scattering clutter attributable to variations in Liquid Water Content (LWC) across a cloud should be added to CLDSIM if measurements of LWC can be extracted from the data, and BRDFs with varying LWC are added as well.

Note: PRA is planning an increased number of 30-120 m resolution databases for future releases of the SSGM. Low resolution global databases are planned as well.

BRDFs

1) Correlated line transmission between a cloud and the surrounding atmosphere should be incorporated into CLDSIM.

2) The variety of cloud types available in the SSGM should be increased by adding more BRDFs, or by generating them on-line.

3) Methods of quickly approximating BRDFs should be developed to allow for modeling of complex scattering patterns in optically thin clouds, and other variations due to changes in microphysical properties of clouds.

4) If quick, online calculation of BRDFs is not implemented, CLDSIM's opacity weighting of the BRDF to account for thin clouds should be replaced with an interpolation between the single scattering result and the optically thick result:

$$\rho_{BD}(\tau) = [\rho_{BD}(\tau_{Large}) - S(\tau_{Large})]\,(1-e^{-\tau}) + S(\tau)$$

5) Higher angular resolution should be used in CLDSIM to better capture BRDF variations

in optically thin clouds.

6) New BRDFs should be validated against aircraft measurements where available.

Note: PRA is planning improvements to the cloud droplet distributions, higher spectral and angular resolution, and two new cloud types for future releases of the SSGM.

CLDSIM Calculational Steps

1) Shadowing of cloud pixels from the sun should include obscuration by distance surfaces and not depend just on the pixel's local orientation.

2) Illumination of cloud pixels by other cloud surfaces should be added in more than a diffuse manner. Multiple resolution renderings of the cloud surface may be appropriate for this task.

3) Back illumination of cloud surfaces and multiple scattering in non-slab geometries should be included for clouds with radii of curvature small compared to scattering mean free paths.

4) Beam transmission of terrain backgrounds through clouds should be modified to include forward scattering enhancements.

5) The smearing of terrain clutter upon passing through clouds should be modeled by modulating the terrain clutter in CLDSIM.

6) Sources of atmospheric clutter should be incorporated into CLDSIM as they become available in standard atmospheric codes.

Note: PRA is planning to replace pixels with triangular facets to improve cloud shadowing. They are planning upgrades to CLDSIM's footprinting routines. They are also planning three-stream cloud-over-cloud and cloud-over-terrain models for future releases of the SSGM

CLDSIM as Hosted in the SSGM

1) More information about the meterology behind the cloud databases should be provided to the SSGM user to aid in correctly positioning them.

2) More robust error checking should be applied to CLDSIM inputs to insure correct atmospheric profiles and cloud types for a given scenario.

3) Changes should be made in the CLDSIM architecture so that only pixels in the FOV are processed.

Note: PRA is reorganizing CLDSIM for speed and will at some point include a "cookie cutter" model to allow one to trim cloud databases for specific applications.

6. REFERENCES

Albright, P.C., 1992, "BASS Meeting Backgrounds Subpanel," presented at the BASS Meeting, Burlington, MA, October 15-16, 1992.

Blasband, C. and J. Jafolla, 1990, "A Comparison of Predicted Cloud Radiance and Measured Data in the Infrared," presented at the Cloud Impacts on DoD Operations and Systems Conference, Monterey, CA, January 1990.

DeVore, J., ATHENA User's Guide, PRi-SB-87-R003, Physical Research, Inc. (1987).

Hansen, J.E., 1971, "Multiple Scattering of Polarized Light in Planetary Atmospheres. Part II. Sunlight Reflected by Terrestrial Water Clouds," J. Atmos. Sci. 28, pp. 1400-1426.

Mertz, F.C., et al., 1991a, BSTS Reference Scene, Natural Background and Target Data Bases.

Mertz, F.C., et al., 1991b, "Validation of a Cloud Scene Simulation Model Using NOAA Multi-spectral Imagery," presented at the Cloud Impacts on DoD Operations and Systems conference, Los Angeles, CA, (July 1991).

Mertz, F.C., 1993, "Phenomenology Component Development: Terrain / Cloud / Atmosphere," PRA B-047-93, Photon Research Associates, presented at the SSGM Developers Meeting, (March 1993).

Shanks, J.G., 1991, "Specular Scattering from Cirrus Clouds: A First-Order Model," presented at the Cloud Impacts on DoD Operations and Systems Conference, Los Angeles, CA, (July 1991).

Shanks, J.G., et al., 1992a, "DSP Response to Background Imagery: Measured and Modeled", presented at the 1992 Meeting of the IRIS Specialty Group on Targets, Backgrounds and Discrimination, Orlando, FL, (January 1992).

Shanks, J.G., 1992b, "SWIR Background Radiance: Expected Distribution for the BP Constellation," briefing given on February 12, 1992.

Shanks, J.G., and F.C. Mertz, 1993, "Terrain and Cloud Component Review," PRA B-141-93, Photon Research Associates, presented at the SSGM Workshop, (August 4-5, 1993).

Stephens, G.L., 1978, "Radiation Profiles in Extended Water Clouds. I: Theory," J. Atmos. Sci, 35, pp. 2111-2122.

Thomas, M.E. and D.D. Duncan, 1993, "Atmospheric Transmission", in Atmospheric Propagation of Radiation, F.G. Smith, ed., volume 2 of The IR/EO Systems Handbook, J.S. Accetta and D.L. Shumaker, Executive Editors (Infrared Information Analysis Center, Environmental Research Institute of Michigan, Ann Arbor, MI, 1993), pp. 105-109.